



NASA Contractor Report 4614

Evaluation of GPS Position and Attitude Determination for Automated Rendezvous and Docking Missions

*Marc D. DiPrinzio and Robert H. Tolson
The George Washington University, Joint Institute for Advancement of Flight Sciences,
Langley Research Center • Hampton, Virginia*

National Aeronautics and Space Administration
Langley Research Center • Hampton, Virginia 23681-0001

Prepared for Langley Research Center
under Cooperative Agreement NCC1-104

July 1994

Abstract

The use of the Global Positioning System for position and attitude determination is evaluated for an automated rendezvous and docking mission. The typical mission scenario involves the chaser docking with the target for resupply or repair purposes, and is divided into three sections. During the homing phase, the chaser utilizes Coarse Acquisition pseudorange data to approach the target; guidance laws for this stage are investigated. In the second phase, differential carrier phase positioning is utilized. The chaser must maintain a quasi-constant distance from the target, in order to resolve the initial integer ambiguities. Once the ambiguities are determined, the terminal phase is entered, and the rendezvous is completed with continuous carrier phase tracking. Attitude knowledge is maintained in all phases through the use of the carrier phase observable. A Kalman filter is utilized to estimate all states from the noisy measurement data. The effects of Selective Availability and cycle slips are also investigated.

Table of Contents

Abstract	1
Nomenclature	4
List of Abbreviations	5
List of Figures	5
List of Tables	7
1. Introduction	8
1.1. The Global Positioning System	8
1.1.1. System Overview	8
1.1.2. The GPS Signal	8
1.1.3. The GPS Observables	9
1.1.3.1. Pseudorange	9
1.1.3.2. Carrier Phase	10
1.1.3.3. Differential GPS	10
1.2. Scope of the Investigation	11
1.2.1. The Nominal Mission	11
1.2.2. Simulation Method	12
1.2.3. Investigation Objectives	13
2. Position Determination from Pseudorange Measurements	13
2.1. Homing Phase Overview	13
2.2. Orbital Mechanics	13
2.2.1. Target and Chaser	13
2.2.2. Chaser Maneuvers	14
2.2.3. GPS Satellites	15
2.3. Line of Sight Determination	16
2.4. SV Selection	18
2.5. Selective Availability	20
2.5.1. Overview	20
2.5.2. SA Residual Generation and Incorporation	21
2.5.3. The Non-Stationarity of Selective Availability	21
2.6. Position Triangulation	21
2.7. The Kalman Filter	23
2.7.1. Filtering Procedure	23
2.7.2. Starting Requirements	24
2.7.3. Correlated Pseudorange Measurement Errors	25
2.7.4. Covariance Consistent, Random Vectors	26
2.8. Maneuvering Errors	26
2.9. Pseudorange Results	28
2.9.1. Simulation Integrity	28
2.9.2. Position Knowledge and Monte Carlo Verification	29
2.9.3. Homing Phase State Knowledge, SA Active	30
2.9.4. Guidance Strategies	31
2.9.5. Effects of Modeling SA Measurement Noise Incorrectly	34
2.10. Homing Phase Conclusions	35

3. Stationkeeping via Differential GPS.....	35
3.1. Overview.....	35
3.2. Differential GPS and the Integer Ambiguity	36
3.3. Kinematic on the Fly GPS and Kalman Filtering	38
3.3.1. Starting Requirements	40
3.3.2. Correlated Phase Measurement Errors	41
3.4. GPS Satellite Tracking	41
3.5. Stationkeeping Results.....	42
3.5.1. State Knowledge: 15° Measurement Noise	42
3.5.2. State Knowledge: 5° Measurement Noise	43
3.5.3. GPS Satellite Usage: 3, 5, and 7 SVs	45
3.6. Stationkeeping Conclusions.....	47
4. Terminal Approach via Differential GPS	48
4.1. Overview.....	48
4.2. GPS Satellite Tracking	48
4.3. Kinematic on the Fly GPS and Terminal Filtering	49
4.4. Corrective Maneuvers.....	49
4.5. Terminal Phase Results.....	49
4.5.1. State Knowledge, No Cycle Slips.....	49
4.5.2. Cycle Slips	51
4.6. Terminal Phase Conclusions.....	54
5. GPS Attitude Determination.....	54
5.1. Overview.....	54
5.2. Attitude Equations of Motion	55
5.3. Carrier Phase Measurements	56
5.4. Attitude Determination from Carrier Phase Measurements	56
5.5. The Attitude Kalman Filter.....	60
5.6. Attitude Results	61
5.6.1. Two Receiver Investigation	61
5.6.1.1. The Use of More GPS Satellites.....	65
5.6.1.2. Increasing the Phase Measurement Accuracy.....	65
5.6.2. Three Receiver Investigation	66
5.6.2.1. Phase Measurement Capacity: 15°	67
5.6.2.2. Phase Measurement Capacity: 5°	68
5.7. Attitude Determination Conclusions	69
6. Summary and Recommendations	69
Appendix A: Description of Computer Programs	71
A.1. Overview.....	71
A.2. Alphabetical Subroutine List and Description	73
References.....	82

Nomenclature

$\hat{}$	estimate
$\bar{}$	truth
$\hat{}$	unit vector
$ $	determinant
$\ \ $	norm
x_0	initial (i.e., $x_0 =$ initial x)
i	inertial frame (i.e., $x_i = x$ expressed in the inertial frame)
tof	target orbital frame (i.e., $x_{tof} = x$ expressed in the target orbital frame)
$\varphi_{x \rightarrow y}$	direction cosine matrix from frame x to frame y (i.e., $\varphi_{tof \rightarrow i} =$ DCM from orbital to inertial frame)
$\delta\Delta\phi$	attitude determination: differential phase difference
$\Delta\phi$	position determination: phase difference ($\Delta\phi = \Delta\phi_0 + \Delta\phi_N$)
$\Delta\phi_0$	position determination: measured phase difference ($0 < \Delta\phi_0 < 2\pi$), attitude determination: nominal phase difference
$\Delta\phi_N$	position determination: whole cycle phase count
λ	GPS carrier wavelength (~ 19.0 cm)
ρ	density
ρ	GPS SV position = (X,Y,Z)
θ	mask angle, phase measurement angle
ω	GPS carrier circular frequency
ϕ	phase measurement
α	mask angle, partial derivative
σ	standard deviation
Φ	state transition matrix
Δt	clock bias
ΔV	velocity increment
Δz	measurement residual
a	antenna phase center position
a_p	acceleration due to drag
\mathbf{b}	baseline vector
$m/(C_D A)$	ballistic coefficient
\mathbf{H}	observation matrix
\mathbf{h}	unit vector to GPS satellite
I	moment of inertia
\mathbf{I}	identity matrix
\mathbf{K}	Kalman gain matrix
\mathbf{k}	wave vector
\mathbf{M}	external torque
n	orbital angular velocity

$N^{(i,j)}$	$i^{\text{th}}, j^{\text{th}}$ integer ambiguity difference
p	pitch
\mathbf{P}	state covariance matrix
\mathbf{Q}	state noise matrix
R	pseudorange
\mathbf{R}	measurement noise matrix
r	normally distributed random number, range from receiver to SV, roll
\mathbf{r}	receiver position = (x,y,z)
t	time
\mathbf{x}	state vector
T	perturbing torque
\mathbf{v}	measurement noise vector
V	velocity
\mathbf{w}	state noise vector
y	yaw
\mathbf{z}	measurement vector

List of Abbreviations

AFB	Air Force Base
C/A	Coarse Acquisition
CSOC	Consolidated Space Operations Center
DCM	Direction Cosine Matrix
GPS	Global Positioning System
P-code	Precision code
PRN	Pseudo Random Noise
RSS	Root Sum Square
SPS	Standard Positioning Service
STM	State Transition Matrix
SV	GPS Satellite Vehicle

List of Figures

Figure 1.2.1.a: The Nominal Rendezvous Scenario (not to scale).....	11
Figure 2.2.1.a: The Target Orbital Frame	14
Figure 2.3.1.a: Line of Sight with Mask Angle Construction.....	17
Figure 2.4.1.a: Typical Minimum and Sub-Optimal GDOP Values.....	19
Figure 2.4.2.a: Typical SV Usage	20
Figure 2.9.1.a: Effect of Constellation Size on SV Observability	29
Figure 2.9.1.b: Effect of Elevation Angle on SV Observability	29
Figure 2.9.3.a: Homing Phase Position Knowledge and Residual	31

Figure 2.9.3.b: Homing Phase Velocity Knowledge and Residual.....	31
Figure 2.9.4.a: Exaggerated One Burn ΔV Requirements and Control Errors	32
Figure 3.2.1.a. One Dimensional Static Phase Measurement	36
Figure 3.5.1.a: Stationkeeping Position Knowledge and Residual, 15° Measurement Noise	42
Figure 3.5.1.b: Stationkeeping Velocity Knowledge and Residual, 15° Measurement Noise	42
Figure 3.5.1.c: Stationkeeping Ambiguity Knowledge and Residual, 15° Measurement Noise	43
Figure 3.5.2.a: Stationkeeping Position Knowledge and Residual, 5° Measurement Noise	44
Figure 3.5.2.b: Stationkeeping Velocity Knowledge and Residual, 5° Measurement Noise	44
Figure 3.5.2.c: Stationkeeping Ambiguity Knowledge and Residual, 5° Measurement Noise	44
Figure 3.5.3.a: Stationkeeping Position Knowledge and Residual, 5 SVs	45
Figure 3.5.3.b: Stationkeeping Velocity Knowledge and Residual, 5 SVs	45
Figure 3.5.3.c: Stationkeeping Ambiguity Knowledge and Residual, 5 SVs	46
Figure 3.5.3.d: Stationkeeping Position Knowledge and Residual, 3 SVs	46
Figure 3.5.3.e: Stationkeeping Velocity Knowledge and Residual, 3 SVs.....	47
Figure 3.5.3.f: Stationkeeping Ambiguity Knowledge and Residual, 3 SVs.....	47
Figure 4.5.1.a: Terminal Position Knowledge and Residual	50
Figure 4.5.1.b: Terminal Velocity Knowledge and Residual	50
Figure 4.5.1.c: Terminal Integer Ambiguity Knowledge and Residual	50
Figure 4.5.2.a: Terminal Position Knowledge and Residual, Cycle Slip at 118 Minutes	51
Figure 4.5.2.b: Terminal Phase Measurement Residual	52
Figure 4.5.2.c: Terminal Position Knowledge and Residual, Repaired Cycle Slip	53
Figure 4.5.2.d: Terminal Integer Ambiguity Knowledge and Residual, Repaired Cycle Slip.....	53
Figure 4.5.2.e: Terminal Measurement Residual, Repaired Cycle Slip.....	53
Figure 5.6.1.a: Homing Attitude Knowledge and Residual, Roll Aligned Antenna	62
Figure 5.6.1.b: Stationkeeping Attitude Knowledge and Residual, Roll Aligned Antenna.....	62
Figure 5.6.1.c: Terminal Attitude Knowledge and Residual, Roll Aligned Antenna.....	62
Figure 5.6.1.d: Homing Attitude Knowledge and Residual, Yaw Aligned Antenna.....	63
Figure 5.6.1.e: Stationkeeping Attitude Knowledge and Residual, Yaw Aligned Antenna.....	63
Figure 5.6.1.f: Terminal Attitude Knowledge and Residual, Yaw Aligned Antenna.....	63
Figure 5.6.1.g: Homing Attitude Knowledge and Residual, Pitch Aligned Antenna.....	64
Figure 5.6.1.h: Stationkeeping Attitude Knowledge and Residual, Pitch Aligned Antenna.....	64
Figure 5.6.1.i: Terminal Attitude Knowledge and Residual, Pitch Aligned Antenna.....	64
Figure 5.6.1.1.a: Stationkeeping Attitude Knowledge and Residual, 6 GPS SVs.....	65

Figure 5.6.1.2.a: Homing Attitude Knowledge and Residual, 5° Measurement Noise	66
Figure 5.6.1.2.b: Stationkeeping Attitude Knowledge and Residual, 5° Measurement Noise	66
Figure 5.6.1.2.c: Terminal Attitude Knowledge and Residual, 5° Measurement Noise	66
Figure 5.6.2.1.a: Homing Attitude Knowledge and Residual, Three Antenna	67
Figure 5.6.2.1.b: Stationkeeping Attitude Knowledge and Residual, Three Antenna	67
Figure 5.6.2.1.c: Terminal Attitude Knowledge and Residual, Three Antenna	68
Figure 5.6.2.2.a: Homing Attitude Knowledge and Residual, Three Antenna	68
Figure 5.6.2.2.b: Stationkeeping Attitude Knowledge and Residual, Three Antenna	69
Figure 5.6.2.2.c: Terminal Attitude Knowledge and Residual, Three Antenna	69

List of Tables

Table 2.4.1.a: Comparison of Optimal and Sub-Optimal SV Selection Efficiencies	20
Table 2.9.2.a: Monte Carlo Verification of Position	29
Table 2.9.4.a: Homing Phase Two Burn Combinations: First Burn Times	33
Table 2.9.4.b: Homing Phase Two Burn Combinations: Second Burn Times	34
Table 2.9.5.a: SA Measurement Noise Analysis	35
Table 3.3.1.a: Satellite Models and Their Observability, Estimating Position and Integer Ambiguity Only	39
Table 6.a: Rendezvous Control Requirements and GPS Knowledge	70

1. Introduction

1.1. The Global Positioning System

1.1.1. System Overview

The Global Positioning System (GPS) is a satellite navigation system that was first proposed in the early 1970's. Primarily, the system was to provide United States military forces with accurate time and position information anywhere on the globe, at any time, and in any weather. Since then, the civilian applications of the system have grown and will continue to grow beyond anything the original designers intended. As it was originally conceived, the system was to consist of a constellation of 24 satellite vehicles (SVs), 21 of which were active with 3 on-orbit spares. With the design and testing phases complete, the system is currently being deployed by the United States, and at the time of this writing a total of 26 operational satellites, of varying ages and capabilities, are in orbit.

Each GPS satellite broadcasts a unique signal from which a user with the proper equipment can determine accurate time and position information. At its most basic level, these signals consist of the positions of the individual GPS satellites; thus, the user position can be determined from a simple triangulation. In most cases, the user desires three dimensional position knowledge, so at least three GPS satellite signals must be in view to meet this need. However, because the user clock will generally not be synchronized with GPS time, this adds an extra unknown so that at least four GPS satellites must be in view for position and time knowledge. Of course, more than four satellites may be used to provide a more robust solution.

The requirement that four GPS satellites be in view dictates the number of satellites that must be in the constellation. When deployed in six equally spaced 12 hour orbits, the minimum number of satellites considered necessary to provide adequate coverage is 21. A measure of the coverage of a satellite constellation is its *constellation value*, which represents the fraction of the Earth and time in which at least four satellites will be in view; for the GPS 21 satellite primary configuration, this value is not to fall below 0.9960.¹ Thus, access to accurate time and position information is available to users over the entire globe, virtually 24 hours a day, in any conditions.

1.1.2. The GPS Signal

The GPS receiver determines the measured travel time of the signal from the GPS satellite through the use of two pseudorandom noise (PRN) codes. The first, the C/A-code (Coarse Acquisition-code), is intended for all users; it is also called the Standard Positioning Service (SPS). The second, the P-code (Precision-code) is intended only for military or other authorized users. The rationale for the two separate codes is security. While the effective wavelength of the C/A-code is 300 m, the P-code is 30 m; thus the civilian C/A-code performance is significantly degraded from the military P-code. In addition, the GPS signal can be intentionally degraded under a policy called Selective Availability (SA), at which point only users with authorized codes can eliminate the added error. This scheme may be invoked, for example, in time of military action so that the enemy may not benefit from the service.²

The GPS signals are broadcast on two carrier frequencies, L1 (1575.42 MHz) and L2 (1227.60 MHz), using spread spectrum techniques so that they are less susceptible to jamming. Both the C/A- and P-codes are modulated on the L1 carrier; however, only the P-code is on the L2 carrier. Again, the intention is to deliberately degrade the C/A performance. Access to two frequencies permits the user to eliminate ionospheric errors, so the P-code solution will be more precise.³

The information contained in the GPS signal, called the navigation message, provides information on the broadcasting satellite, as well as the entire constellation. Over half of the navigation message is dedicated to accurately describing the state of the satellite that broadcast the signal. This includes information on the health of the satellite, the satellite position and velocity, and information to correct for various errors. The remainder of the message contains ephemerides for the rest of the GPS satellites (for quick visibility checks and signal acquirement), health status of the GPS satellites, as well as information reserved for military use.

The control of the GPS SVs is maintained through a worldwide network of ground stations, with the master control station located at the Consolidated Space Operations Center (CSOC) at Falcon AFB, Colorado Springs, Colorado. The main responsibility of the ground segment is to ensure that the information broadcast by the satellites is within operational specifications. Once per day, the monitor stations upload ephemerides and clock information, as determined by the master control station. This, combined with the fact that the satellite clocks are accurate to a few parts in 10^{13} over one day, ensures that the SVs remain synchronized, and can thus provide accurate positioning information.

1.1.3. The GPS Observables

1.1.3.1. Pseudorange

The pseudorange is a timing measurement related to both the signal propagation delay from the satellite to the receiver, and the clock offsets. If the user clock were precisely synchronized with GPS time, then the range to the GPS satellite would be determined by multiplying the propagation delay time (Δt) with the speed of light (c)

$$R = c\Delta t \quad (1)$$

The delay time is calculated through a code correlation of the GPS signal and the internal code generated by the receiver. However, the user and GPS clocks will generally not be synchronized, so the correlation time (Δt) consists of true travel time plus a clock offset component

$$\Delta t = \Delta t_{true} + \Delta t_{clock} \quad (2)$$

Thus, the measurement consists of the true range plus a component due to the clock offsets, hence the name pseudorange

$$R = c(\Delta t_{true} + \Delta t_{clock}) \quad (3)$$

As mentioned above, there are four quantities of interest, three positions and the clock offset. Thus, the four pseudorange equations corresponding to the four GPS satellites must be solved simultaneously; this will yield the user position and clock offset. This process is explored in more detail in Section 2.6, *Position Triangulation*.

1.1.3.2. Carrier Phase

The carrier phase is a second observable available to users of GPS, possessing both advantages and disadvantages. On the positive side, because the GPS wavelength is approximately 19 cm, this results in a significant increase in accuracy over the use of C/A-code or even P-code. However, the implementation of the carrier phase is both more complicated and more sensitive. An event called a cycle slip can occur in practice; this happens when the receiver miscounts the carrier phase, leading to errors in the position knowledge. Still, the general consensus is that the advantages to be gained outweigh the added difficulties.

Consider a GPS carrier phase receiver, immediately after carrier tracking has begun. Due to the cyclical nature of the phase, the instantaneous phase measurement will be in the range 0 to 2π . However, the total phase measurement is given by this value plus some integer number of wavelengths representing the remaining distance to the GPS spacecraft (N). Thus, the phase measurement is described by

$$\phi = \frac{1}{\lambda} (\Delta t_{true} + \Delta t_{clock}) + N \quad (4)$$

where, as with the pseudorange, the measurement reflects both the true range and a range associated with the clock offset. If the integer N were known, then complete position knowledge could be obtained through the continuous tracking of the phase. In general, GPS receivers track the phase by initializing an internal counter to a preset large negative integer. Then, at every positive phase zero crossing, this counter is incremented, yielding knowledge of the number of wavelengths passed since the measurement was begun. Unfortunately, N , termed the initial integer ambiguity, is generally not known. Thus, before the carrier phase information can be of any value, the integer ambiguity must be resolved. Several methods are available for performing this task, all of which are described in more detail in Section 3.2, *Differential GPS and the Integer Ambiguity*.

1.1.3.3. Differential GPS

When dealing with two or more GPS receivers in "close" proximity, it is important to realize that many of the errors present in the signal are common to both receivers when the same GPS satellites are used for triangulation. The definition of close, in this sense, must be evaluated on a case by case basis, dependent on the particular requirements in question. One example of a common error is the ionospheric and tropospheric delays in the GPS signal. In addition, Selective Availability errors can also be considered common to receivers relatively close together. When dealing with such errors, higher accuracy results can be obtained by utilizing differential GPS. This mode of operation entails subtracting the measurements of one receiver (pseudorange or phase)

from another, thereby obtaining a relative measure of position. In this way, common errors are eliminated in the differencing process.

1.2. Scope of the Investigation

This study is primarily intended to benefit automated rendezvous missions where the chaser is some type of unmanned craft, and the target is cooperative. The term cooperative in this sense basically means that the target is broadcasting all necessary GPS information to the chaser. Most likely, these types of missions will fall into the resupply or service areas. For example, an increasingly possible scenario is the use of a small, automated craft for the resupply of the International Space Station. Also, the methods explored in research could be applied to the capture and repair of a malfunctioning satellite, or the refueling of an operative vehicle. In addition, in the wake of the Galileo and Mars Observer failures, it has been proposed to utilize some type of on-orbit inspection craft to test such things as antenna deployment; in this way, necessary repairs can be made before the craft leaves the Earth. Hence, the subjects explored in this investigation are applicable to a wide variety of rendezvous scenarios.

1.2.1. The Nominal Mission

For the purposes of this investigation, the typical simulation will begin assuming the chaser is on-orbit, trailing the target by 50 km. For clarity, a simplified rendezvous sequence is shown in Figure 1.2.1.a below. The first phase of the rendezvous, called the homing phase, begins with a maneuver (ΔV_1) that enters the chaser on a trajectory towards the target. During this phase, C/A pseudoranges will be used to estimate the position of the chaser alone, independent of the target. One or more corrective burns (ΔV_2) may be performed to account for trajectory errors. At the end of the first phase, it is not intended for the chaser to meet the target; rather, the chaser enters a stationkeeping mode a nominal distance behind the target (approximately 2 km). To accomplish this, a burn (ΔV_3) is performed to reduce relative motion between chaser and target.

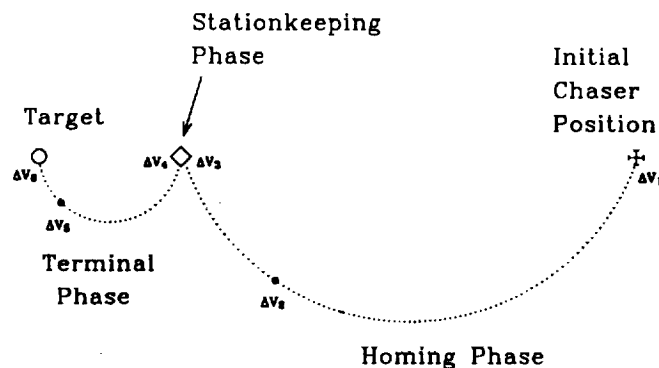


Figure 1.2.1.a: The Nominal Rendezvous Scenario (not to scale)

In the second phase of the rendezvous, the stationkeeping phase, differential GPS with carrier phase positioning is used to gain enhanced relative position knowledge. As mentioned previously, when the carrier phase is used, extra unknowns (the integer ambiguities) must be resolved. Thus, this phase is required solely to initialize the carrier phase positioning. No maneuvers are needed or wanted; a constant chaser position relative to the target is desired as much as possible to hasten the determination of the unknowns.

Once the integer ambiguities are resolved, a maneuver is performed to close the remaining 2 km between the spacecraft (ΔV_4). At this point, the chaser is in the terminal phase of the rendezvous, and any trajectory errors are eliminated through a final corrective burn (ΔV_5). The continuous tracking of the carrier phase will yield highly accurate position and velocity information until the rendezvous is complete (ΔV_6).

During all phases of the mission, carrier phase data is processed to estimate the attitude of the chaser. It is important to note that because of the close proximity of the receivers, it is not necessary to resolve any integer ambiguities in the attitude determination. No attempt has been made to model an attitude control system.

1.2.2. Simulation Method

This simulation utilizes the Kalman filter approach to estimate the state from a series of noisy measurements. While the Kalman filter is a linear filter, some processes in this study (GPS position triangulation) are nonlinear in nature. In addition, the SA signal is non-Gaussian, which complicates the interpretation of the simulation statistics. The equations of motion are linearized in all cases for use with this type of filter; however, whether this approach is valid is a question to be answered by this study.

This simulation uses a "truth" and an "estimate" model to investigate the system of interest. The truth model is based on the propagation of the state via the linearized equations of motion (position and attitude), with state noise added to account for mismodeling of the system. The Kalman estimate of the state is derived from the noisy measurements (pseudorange and phase). Simulation strategies are discussed in more detail in Sections 2.7, *The Kalman Filter*, 3.3, *Kinematic on the Fly GPS and Kalman Filtering*, 4.3, *Kinematic on the Fly GPS and Terminal Filtering*, and 5.5, *The Attitude Kalman Filter*.

One final topic involving the data processing in this investigation should be discussed. During the homing phase, the simulation only processes data from the chaser; the target position and attitude are assumed known. While this obviously will not be the case in a true mission, it is assumed that the target will possess GPS sensors. It then follows that the position and attitude knowledge demonstrated on the chaser in this simulation will be achievable by the target as well. In this case, an estimate of the nominal error (chaser and target) during the homing phase can be obtained by the root-sum-square (RSS) of the two components; this will lead to an increase in the error demonstrated in this investigation by a factor of $\sqrt{2}$. At worst case, the error would be the sum of the two components, leading to a factor of 2 increase in the homing phase results contained herein. Once the homing phase is complete, the chaser and target switch to differential carrier phase positioning, and pseudorange data is no longer processed. In this way, higher accuracy *relative* state information can be obtained. Thus,

because no assumptions are made on the position of the target, the factor of $\sqrt{2}$ is not necessary for the final two phases.

1.2.3. Investigation Objectives

The fundamental question this research seeks to answer is whether two cooperative spacecraft can rendezvous within a prescribed tolerance using GPS alone, i.e. unaided by any other navigation or attitude sensing system. Many specific points to be answered fall under this general question, including:

- Can Kalman filtering yield sufficiently accurate results in all phases of the rendezvous (pseudorange and carrier phase), for both position and attitude sensing?
- How will Selective Availability affect the pseudorange results?
- What type of guidance strategy should be used?
- Can the integer ambiguities be resolved in the orbital situation?
- Will carrier phase positioning provide sufficient state knowledge for terminal rendezvous?
- Could a carrier phase cycle slip lead to catastrophic failure? If so, can a cycle slip be detected and repaired?

All of these topics are investigated and discussed in the sections below.

2. Position Determination from Pseudorange Measurements

2.1. Homing Phase Overview

This phase of the investigation analyzes the position knowledge of the chaser as it homes in on the target, covering the range from ΔV_1 to ΔV_3 in Figure 1.2.1.a. It is assumed that the orbital insertion is performed satisfactorily, with the chaser trailing the target at the specified distance, typically 50 km. Based on the initial knowledge of the chaser's position, a maneuver is performed to initiate the rendezvous. C/A code pseudoranges will be used to determine the chaser position until it arrives within about two kilometers of the target. At user specified intervals, the chaser receives measurement updates perturbed by SA. A Kalman filter is utilized to obtain the optimal estimate of the chaser's position. These estimates are used to calculate the necessary corrective burns to rendezvous with the target. The system models and results are described below.

2.2. Orbital Mechanics

2.2.1. Target and Chaser

This section highlights the mechanics between the target and the chaser. For simplicity, the computations are performed in the target orbital frame. As seen below, this frame is formed with the X-axis *opposite* the target velocity vector, the Y-axis in the radial direction, and the Z-axis normal to the orbital plane.

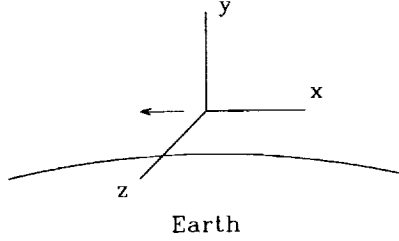


Figure 2.2.1.a: The Target Orbital Frame

For the target orbital frame, the linearized equations of relative motion of the chaser assuming the target is in a circular orbit are⁴

$$\begin{aligned}\ddot{x} - 2n\dot{y} &= 0 \\ \ddot{y} + 2n\dot{x} - 3n^2y &= 0 \\ \ddot{z} + n^2z &= 0\end{aligned}\quad (5)$$

where n is the orbital angular velocity. The solution of these equations from $t=0$ to t is⁵

$$\begin{bmatrix} x \\ y \\ z \\ \dot{x} \\ \dot{y} \\ \dot{z} \end{bmatrix} = \begin{bmatrix} 1 & 6(nt - \sin nt) & 0 & -3t + \frac{4}{n}\sin nt & \frac{2}{n}(1 - \cos nt) & 0 \\ 0 & 4 - 3\cos nt & 0 & \frac{2}{n}(-1 + \cos nt) & \frac{1}{n}\sin nt & 0 \\ 0 & 0 & \cos nt & 0 & 0 & \frac{1}{n}\sin nt \\ 0 & 6n(1 - \cos nt) & 0 & -3 + 4\cos nt & 2\sin nt & 0 \\ 0 & 3n\sin nt & 0 & -2\sin nt & \cos nt & 0 \\ 0 & 0 & -n\sin nt & 0 & 0 & \cos nt \end{bmatrix} \begin{bmatrix} x_0 \\ y_0 \\ z_0 \\ \dot{x}_0 \\ \dot{y}_0 \\ \dot{z}_0 \end{bmatrix}\quad (6)$$

Thus, given the position and velocity of the chaser relative to the target, the chaser's position at a later time t is given to first order by this equation. For this simulation, the time period of interest is in between measurements, or $t = \Delta t$. It should be noted that the matrix in the above equation is the state transition matrix used in the Kalman filter; this will be explored in more detail in later sections.

2.2.2. Chaser Maneuvers

Given an initial position x_0, y_0, z_0 , it is possible to determine the velocities necessary to arrive at the origin in a specified time τ . The solution to the linearized equations can be inverted to yield the following conditions⁶

$$\begin{aligned}
\dot{x}_0 &= \frac{x_0 \sin n\tau + y_0 [6n\tau \sin n\tau - 14(1 - \cos n\tau)]}{3\tau \sin n\tau - 8(1 - \cos n\tau) / n} \\
\dot{y}_0 &= \frac{2x_0(1 - \cos n\tau) + y_0(4 \sin n\tau - 3n\tau \cos n\tau)}{3\tau \sin n\tau - 8(1 - \cos n\tau) / n} \\
\dot{z}_0 &= \frac{-z_0 n}{\tan n\tau}
\end{aligned} \tag{7}$$

When there is a burn (such as at the start of the simulation), the true and estimate velocity increments must be determined. Based on the above equations, the velocities to arrive at the origin are calculated based on the current *estimate* of position, because the true position is not known. The velocity estimate after the maneuver becomes the nominal value calculated from the equations above. The true velocity is set to this nominal velocity plus terms accounting for errors in the burn.

To account for maneuver execution errors, two parameters are used which describe duration and direction errors in the burn. Duration, or magnitude, errors can be attributed to burn time errors, incorrect specific impulses, and the like. These errors are modeled through the use of the standard deviation of the magnitude error, an input parameter assumed to be known at the start of the simulation. Direction errors could be due to thruster misalignment, spacecraft attitude errors, and so forth. These effects are modeled through the standard deviation of the error in the two directions perpendicular to the burn axis. A numerical value is obtained from the root-sum-square (RSS) of two components. The first is a floor ΔV direction error, representing thruster misalignment. This is an input parameter, and can be changed to investigate a variety of thruster accuracies. For this study, this value is nominally set at 0.01° . The second component is obtained from the attitude knowledge at the time of the maneuver. The rationale for this is that if the attitude is known only to a certain degree, then the accuracy of the pointing of the ΔV cannot be any better than that. The actual procedure to determine the true velocity increments is described in Section 2.8, *Maneuvering Errors*. Through the use of these methods, effects of errors in thrusting can be investigated.

2.2.3. GPS Satellites

Whereas the calculations for the target and chaser were performed in the orbital frame, the GPS processing was carried out in an inertial frame fixed at the Earth's center. The GPS satellite orbits were propagated using universal variables⁷. In order to avoid having to recalculate the GPS states every simulation, a pre-processing program was written that accepts the orbital elements for the constellation and constructs a table for subsequent utilization. In this way, the GPS orbit prediction need only be performed once for each constellation, thus building a library of GPS state tables. For example, one data file may have a 16 satellite constellation, and another may have 21 satellites. The constellation used to obtain the results in this investigation consisted of an optimal 21 satellite configuration⁸.

In addition, given the orbital elements of the target, its ephemerides are propagated and stored via the pre-processing. Any conversion between inertial and local

frames is performed through the use of the direction cosine matrix (DCM). For example, the inertial position of the chaser in terms of the target orbital frame is

$$\mathbf{r}_i^{chaser} = \mathbf{r}_i^{origin} + \Phi_{tof \rightarrow i} \mathbf{r}_{tof}^{chaser} \quad (8)$$

This equation states that the inertial position of the chaser equals the inertial position of the origin of the orbital frame plus the DCM from the orbital to inertial coordinates times the chaser position in orbital coordinates. For a circular orbit, the DCM is found from the relation

$$\Phi_{tof \rightarrow i} = \begin{bmatrix} \frac{-\dot{\mathbf{r}}}{\|\dot{\mathbf{r}}\|} & \frac{\mathbf{r}}{\|\mathbf{r}\|} & \frac{-\dot{\mathbf{r}}}{\|\dot{\mathbf{r}}\|} \times \frac{\mathbf{r}}{\|\mathbf{r}\|} \end{bmatrix} \quad (9)$$

where \mathbf{r} is the position of the body in inertial coordinates. Likewise, when converting from inertial to orbital coordinates, the orbital position is found from

$$\mathbf{r}_{tof}^{chaser} = \Phi_{i \rightarrow tof} (\mathbf{r}_i^{chaser} - \mathbf{r}_i^{origin}) \quad (10)$$

where the direction cosine matrices are related by

$$\Phi_{i \rightarrow tof} = \Phi_{tof \rightarrow i}^T \quad (11)$$

Thus, given any inertial position, these relations permit the conversion into orbital coordinates, and vice versa.

2.3. Line of Sight Determination

GPS receivers have software that selects the optimal set of GPS satellites with which to determine the current position. Before this can be carried out, the line of sight to all satellites must be determined for the time periods of interest. In addition, it was desired to include the capability to set a mask angle from the surface of the Earth (nominally 5°), in order to model the reduced visibility through the atmosphere near the horizon. This section highlights the method used to determine receiver-satellite line of sight. Once the chaser orbital coordinates are transformed into inertial coordinates, the following process is carried out for every SV.

- a) If the component of the SV position in the direction of the chaser is greater than the radius of the chaser, then the SV must be in sight, and the line of sight process is complete; otherwise, continue to step b. The SV position in the direction of the chaser is found from

$$SV_{chaser} = \|\mathbf{r}_{SV}\| \left(\frac{\mathbf{r}_{chaser} \cdot \mathbf{r}_{SV}}{\|\mathbf{r}_{chaser}\| \|\mathbf{r}_{SV}\|} \right) \quad (12)$$

b) Determine whether a line connecting the chaser and the SV positions crosses the Earth's surface (assumed to be a sphere). If this is true, the SV is *not* in sight, and the line of sight determination process is ended; otherwise continue to step c. The line of sight crosses the Earth's surface if the shortest distance between the line and the origin (the center of the earth) is less than the radius of the Earth. The distance from the origin to the line

$$\frac{x-x_1}{a_x} = \frac{y-y_1}{a_y} = \frac{z-z_1}{a_z} \quad (13)$$

where \mathbf{a} is the direction vector

$$\mathbf{a} = [x_2 - x_1 \quad y_2 - y_1 \quad z_2 - z_1]^T \quad (14)$$

is given by⁹

$$d = \frac{\|\mathbf{u} \times \mathbf{a}\|}{\|\mathbf{a}\|} \quad (15)$$

where $\mathbf{u} = [-x_1 \quad -y_1 \quad -z_1]^T$.

c) From the known receiver and SV positions, construct the following figure:

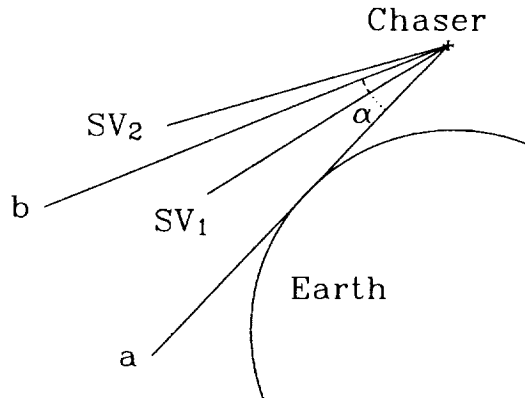


Figure 2.3.1.a: Line of Sight with Mask Angle Construction

where α is the mask angle. Three unit vectors are calculated: first, from the chaser to the point of tangency on the Earth (\mathbf{a}), second, from the chaser along the line formed when the Earth tangent is rotated to the desired mask angle (\mathbf{b}),

and third, from the chaser to the SV (\mathbf{SV}_1 or \mathbf{SV}_2). The two cross products $\mathbf{a} \times \mathbf{SV}$ and $\mathbf{SV} \times \mathbf{b}$ are evaluated; if they are both the same sign, then the SV is *not* in view due to the mask angle. For example, these cross products are the same sign for \mathbf{SV}_1 in Figure 2.3.1.a, so it is not in sight due to the mask angle. On the other hand, \mathbf{SV}_2 will yield cross products of opposite signs, so it is in sight. This process must be performed for every SV at every time step to yield the required line of sight information.

2.4. SV Selection

The minimum number of SVs required to determine the user's coordinates via pseudorange data without any prior information is four, to account for the three position coordinates and the receiver clock offset from GPS time (see Section 2.6, *Position Triangulation*). The choice of the best four satellites out of the n SVs in view is very critical, because it directly relates to the accuracy of the solution. The optimal choice is a function of several variables, including geometry, signal strength, health of the SV, and so forth. Currently, the simulation only takes into account the geometry of any given triangulation; however, it is possible to enhance the programming and include these other effects as well.

This simulation utilizes the Geometric Dilution of Precision (GDOP) as the standard of selection of any four satellites. The GDOP is basically a "measure of goodness" of the geometry of any particular GPS solution; it can be thought of as the inverse of the volume formed by the four SVs and the receiver. Thus, if the SVs are all almost directly overhead of the receiver, then the volume would be small, and the GDOP high, implying a poor geometry. However, if one of the SVs was overhead, and the other three were all at a low inclination to the chaser and equally spaced at 120° apart, the volume would be close to the maximum, implying a very low, and very desirable, GDOP.

The formula for calculation of GDOP is

$$GDOP = \frac{\sqrt{\sum_{i=1}^4 (b_i^2 + 9v_i^2)}}{3V} \quad (16)$$

where V is the volume of the tetrahedron formed after connecting the endpoints of four unit vectors pointing from the receiver to their respective i^{th} satellite, b_i is the area of the i^{th} lateral face of the endpoint tetrahedron, and v_i is the volume of the tetrahedron formed by the i^{th} lateral face of the endpoint tetrahedron and the receiver location¹⁰. Note that the area of a triangle with the vertices P_1, P_2, P_3 is given by¹¹

$$A = \left\{ \frac{1}{4} \left(\left| \begin{array}{ccc} y_1 & z_1 & 1 \\ y_2 & z_2 & 1 \\ y_3 & z_3 & 1 \end{array} \right|^2 + \left| \begin{array}{ccc} z_1 & x_1 & 1 \\ z_2 & x_2 & 1 \\ z_3 & x_3 & 1 \end{array} \right|^2 + \left| \begin{array}{ccc} x_1 & y_1 & 1 \\ x_2 & y_2 & 1 \\ x_3 & y_3 & 1 \end{array} \right|^2 \right) \right\}^{1/2} \quad (17)$$

and the volume of the tetrahedron with the vertices P_1, P_2, P_3, P_4 is¹²

$$V = \frac{1}{6} \begin{vmatrix} x_1 & y_1 & z_1 & 1 \\ x_2 & y_2 & z_2 & 1 \\ x_3 & y_3 & z_3 & 1 \\ x_4 & y_4 & z_4 & 1 \end{vmatrix} \quad (18)$$

It is possible to evaluate every combination of four of the n SVs in view, and then choose the combination that yields the minimum GDOP. The number of evaluations of n SVs taken 4 at a time is given by the binomial coefficient¹³

$$N = \binom{n}{4} = \frac{n!}{(n-4)!4!} \quad (19)$$

so that as the number SVs in view increases above four, the necessary number of function evaluations increases rapidly. To reduce this computational requirement, a sub-optimal GDOP selection criterion¹⁴ has been incorporated. The process involves determining the three *separate* GPS satellites that satisfy the following criteria. The vector from the receiver to the first SV has the greatest component along the radial direction of the receiver; the vector from the receiver to the second SV has the greatest component opposite the receiver's velocity vector, and the vector from the receiver to the third SV has the greatest component perpendicular to the above two vectors. Finally, for each of the remaining satellites, the GDOP is calculated with the above three SVs, and the resulting minimum is selected. Fundamentally, this procedure ensures that three of the four SVs will be chosen so as to form a nearly orthogonal set of axes, resulting in a large enclosed volume, and hence a small GDOP. In practice, this procedure achieves GDOP values on average about 1.5 times the minimum. This is illustrated in Figure 2.4.1.a, which shows the minimum and sub-optimal minimum GDOP values for a typical rendezvous scenario over one orbit of the target.

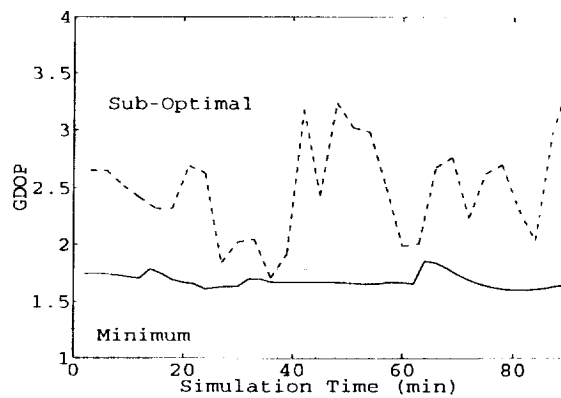


Figure 2.4.1.a: Typical Minimum and Sub-Optimal GDOP Values

The most important aspect of this method, however, is that it requires only $n - 2$ GDOP evaluations. The computational savings are shown in Table 2.4.1.a.

Table 2.4.1.a: Comparison of Optimal and Sub-Optimal SV Selection Efficiencies

Number of SVs in Sight	Optimal GDOP Evaluations	Sub-Optimal GDOP Evaluations
5	5	2
6	15	3
7	35	4
8	70	5
9	126	6
10	210	7

A point to emphasize about this SV selection method is that from one time step to the next ($\Delta t = 3$ min), the chosen four satellites rarely remain the same. This is a positive trait in the sense that it virtually ensures independent measurements at every pseudorange epoch. On the other hand, this method requires that the pseudorange receiver maintain a lock on all satellites in view. For illustrative purposes, a typical plot of SV usage over one orbit is shown on Figure 2.4.2.a. A dot means that the satellite is in view, and a circle means that the satellite is in use.

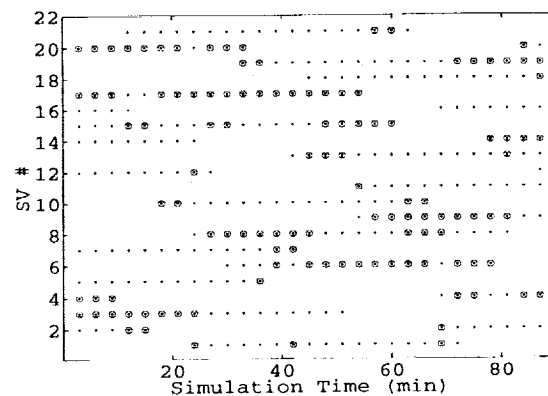


Figure 2.4.2.a: Typical SV Usage

2.5. Selective Availability

2.5.1. Overview

It was desired to investigate the effects that Selective Availability may have on performing an automated rendezvous mission; thus, an SA model is included. Numerous studies have simulated SA statistically; for example, some models assume that the pseudorange error due to SA is an exponentially correlated random variable with a time constant of 15 minutes¹⁵. Other models have attempted to account for both "orbit SA" (perturbed GPS SV ephemerides reported to the receiver), and "dither SA" (false drift of the SV clocks)¹⁶. In this case, both effects are modeled as second order Markov processes, with correlation times of 3 and 60 minutes, respectively. This simulation utilizes an SA model based on actual GPS data developed by Braasch¹⁷. The advantage

that this model has above the statistical approaches above is that it was derived from actual GPS data.

2.5.2. SA Residual Generation and Incorporation

The procedure for simulating SA is begun by obtaining an actual sample of pseudorange data from one GPS satellite. With only one SV, the issue of the receiver clock offset from GPS time poses a problem. If a highly stable crystal oscillator is used, the clock offset could be represented by a first order polynomial. Then, the residuals are calculated by subtracting the best fitting straight line from the collected data. Braasch states that these residuals primarily represent SA because the variance due to SA is two orders of magnitude greater than all other error sources. It is important to realize that this method will not identify a non zero mean component of SA.

Once the SA residual time series is collected, an optimum filter $G(\omega,t)$ can be constructed such that when the data is passed through it, the output is white noise with variance σ^2 . Next, the inverse of $G(\omega,t)$, $H(\omega,t)$, is determined. Finally, *statistically equivalent* SA residual data is acquired by passing white noise with variance σ^2 through the inverse filter. Fundamentally, this procedure reduces to producing a time series whose power spectrum is the same as the original signal. In this way, an arbitrary amount of SA data can be generated for the purpose of this simulation. In addition, it is very easy to modify the filter parameters should new pseudorange data indicate a change in the nature of the SA signal.

The incorporation of this model into the simulation is straightforward. The necessary length of SA data for each GPS satellite is calculated according to the procedure described above. This simulation investigates two levels of SA measurement noise, 27 m and 39 m, as described by Braasch. Then, when the GPS pseudoranges are calculated, the SA error corresponding to the correct SV and time is simply added to that pseudorange. These perturbed pseudoranges are then entered into the triangulation routine to determine the position estimate, which is biased by SA. These are the measurements used by the Kalman filter to optimally estimate the state.

2.5.3. The Non-Stationarity of Selective Availability

A process is said to be stationary if its statistical properties do not vary with the passing of time. The model used in this investigation assumes that the SA residual data is stationary. However, in a more recent paper¹⁸ additional SA data samples were analyzed, and it was determined that several of the records did exhibit non-stationary characteristics. Unfortunately, this complicates the modeling of SA; instead of simply modeling a system with constant coefficients, the coefficients now change with time. On a positive note, the recently collected data did exhibit stationarity for periods of up to one and a half hours. As a result, it will be assumed that the current SA model will be valid for the time periods of interest.

2.6. Position Triangulation

The final operation involves the position triangulation from GPS pseudoranges; this basically follows the standard procedure¹⁹. With the four GPS satellite positions (X_i ,

Y_i, Z_i) and the four simultaneous pseudorange measurements (R_i), the user position (x, y, z) and clock bias (Δt) can be determined from the simultaneous solution of

$$(R_i - c\Delta t)^2 = (x - X_i)^2 + (y - Y_i)^2 + (z - Z_i)^2 \quad i = 1..4 \quad (20)$$

The solution involves linearizing these equations, and applying Newton's method. Given an a priori estimate of the chaser's state ($\hat{x}, \hat{y}, \hat{z}, \hat{\Delta t}$) the corrections to this a priori estimate ($\delta x, \delta y, \delta z, \delta \Delta t$) can be computed by first expanding the measurement equations and keeping only first order terms, so that

$$R_i = \hat{R}_i + \frac{\partial \hat{R}_i}{\partial \hat{x}} \delta x + \frac{\partial \hat{R}_i}{\partial \hat{y}} \delta y + \frac{\partial \hat{R}_i}{\partial \hat{z}} \delta z + \frac{\partial \hat{R}_i}{\partial \hat{\Delta t}} \delta \Delta t \quad i = 1..4 \quad (21)$$

The partial derivatives are given by

$$\begin{aligned} \frac{\partial \hat{R}_i}{\partial \hat{x}} &= \frac{\hat{x} - X_i}{\hat{r}_i} = \alpha_{i1} & \frac{\partial \hat{R}_i}{\partial \hat{z}} &= \frac{\hat{z} - Z_i}{\hat{r}_i} = \alpha_{i3} \\ \frac{\partial \hat{R}_i}{\partial \hat{y}} &= \frac{\hat{y} - Y_i}{\hat{r}_i} = \alpha_{i2} & \frac{\partial \hat{R}_i}{\partial \hat{\Delta t}} &= c = \alpha_{i4} \end{aligned} \quad (22)$$

where

$$\hat{r}_i = \sqrt{(\hat{x} - X_i)^2 + (\hat{y} - Y_i)^2 + (\hat{z} - Z_i)^2} \quad (23)$$

Thus, the problem can be formulated as the matrix equation

$$\begin{bmatrix} \alpha_{11} & \alpha_{12} & \alpha_{13} & \alpha_{14} \\ \alpha_{21} & \alpha_{22} & \alpha_{23} & \alpha_{24} \\ \alpha_{31} & \alpha_{32} & \alpha_{33} & \alpha_{34} \\ \alpha_{41} & \alpha_{42} & \alpha_{43} & \alpha_{44} \end{bmatrix} \begin{bmatrix} \delta x \\ \delta y \\ \delta z \\ \delta \Delta t \end{bmatrix} = \begin{bmatrix} R_1 - \hat{R}_1 \\ R_2 - \hat{R}_2 \\ R_3 - \hat{R}_3 \\ R_4 - \hat{R}_4 \end{bmatrix} \quad (24)$$

or

$$\mathbf{A} \delta \mathbf{u} = \delta \mathbf{R} \quad (25)$$

so that

$$\delta \mathbf{u} = \mathbf{A}^{-1} \delta \mathbf{R} \quad (26)$$

Therefore, the corrections to the a priori estimate $\delta \mathbf{u}$ can be solved for iteratively, until the desired degree of accuracy is achieved. Incidentally, the \mathbf{A}^{-1} matrix is a direct

indicator of the instantaneous geometry of the system, and will be used in the Kalman filter to properly transform the covariance; this is discussed in more detail in the next section.

2.7. The Kalman Filter

2.7.1. Filtering Procedure

Knowing that the GPS pseudoranges have been perturbed by SA and other errors, it is desired to filter these noisy measurements to obtain an optimal estimate of the spacecraft position. A standard Kalman filter is utilized to acquire this estimate, based on the development in Gelb²⁰. As outlined in the introduction, the Kalman filter utilizes a "truth" model and a "knowledge" model. Both models are propagated through the use of the state transition matrix, Φ ; however, the truth model accounts for errors in system modeling by adding a random vector $\bar{\mathbf{w}}$, with zero mean and covariance \mathbf{Q}_k (the state noise). This covariance matrix is an input parameter, so that a variety of system errors can be investigated. The truth model is of the form

$$\bar{\mathbf{x}}_k = \Phi_{k-1} \bar{\mathbf{x}}_{k-1} + \bar{\mathbf{w}}_{k-1} \quad \bar{\mathbf{w}}_k \approx N(\bar{\mathbf{0}}, \mathbf{Q}_k) \quad (27)$$

Note that the state transition matrix, Φ , is the same as described in Section 2.2.1, *Target and Chaser*, except that the state is augmented to account for the receiver clock bias. This investigation assumes that over the time period of interest, there is no drift of the user clocks. Thus, the clock bias term in the state transition matrix is unity.

The measurement for this model is the receiver position calculated from the GPS signals. The measurement equation is of the form

$$\bar{\mathbf{z}}_k = \hat{\mathbf{r}} + \bar{\mathbf{v}}_k \quad \bar{\mathbf{v}}_k \approx N(\bar{\mathbf{0}}, \mathbf{R}_k) \quad (28)$$

It should be made clear that $\hat{\mathbf{r}}$ in the above equation is the position estimate perturbed by SA only. This is calculated by taking the true pseudoranges from the receiver to the GPS satellites and adding the Selective Availability error. Then, these pseudoranges are used to determine the perturbed position measurement, based on the procedure outlined in Section 2.6, *Position Triangulation*; this procedure yields the SA perturbed position vector $\hat{\mathbf{r}}$. This model also includes a noise term \mathbf{v} with mean zero and covariance \mathbf{R}_k (the measurement noise), yielding the noisy measurement vector \mathbf{z} . As with the state noise matrix (\mathbf{Q}_k), \mathbf{R}_k is an input parameter to allow for flexibility in modeling the system.

The measurement noise matrix \mathbf{R}_k must be expressed in terms of the pseudorange errors, because the pseudorange error lies along the line connecting the receiver and the GPS satellite. The geometry of each individual measurement is then converted to inertial coordinates using the \mathbf{A}^{-1} matrix described in the previous section. The proper \mathbf{R}_k is calculated from

$$\mathbf{R}_k = \mathbf{A}^{-1} \mathbf{R}_{k \text{ pseudorange}} \mathbf{A}^{-1T} = \sigma^2 \mathbf{A}^{-1} \mathbf{I} \mathbf{A}^{-1T} = \sigma^2 \mathbf{A}^{-1} \mathbf{A}^{-1T} \quad (29)$$

where \mathbf{R}_k has been assumed to be diagonal (i.e., spherical in pseudorange), with noise variance levels of σ^2 .

As with the truth model, the estimate model utilizes the state transition matrix to propagate the estimate; however, the procedure is slightly different. Starting after a measurement update, the state is propagated until the next measurement via the relation

$$\hat{\mathbf{x}}_k(-) = \Phi_{k-1} \hat{\mathbf{x}}_{k-1}(+) \quad (30)$$

where (+) corresponds to the time after a measurement, and (-) is the time immediately before the next measurement. The error covariance is projected in between measurements by

$$\mathbf{P}_k(-) = \Phi_{k-1} \mathbf{P}_{k-1}(+) \Phi_{k-1}^T + \mathbf{Q}_{k-1} \quad (31)$$

Upon the reception of another measurement, the state and covariance estimates are updated to account for this new information. First, the Kalman gain matrix is computed

$$\mathbf{K}_k = \mathbf{P}_k(-) \mathbf{H}_k^T [\mathbf{H}_k \mathbf{P}_k(-) \mathbf{H}_k^T + \mathbf{R}_k]^{-1} \quad (32)$$

Then, the state and covariance updates are

$$\hat{\mathbf{x}}_k(+) = \hat{\mathbf{x}}_k(-) + \mathbf{K}_k [\mathbf{z}_k - \mathbf{H}_k \hat{\mathbf{x}}_k(-)] \quad (33)$$

$$\mathbf{P}_k(+) = [\mathbf{I} - \mathbf{K}_k \mathbf{H}_k] \mathbf{P}_k(-) \quad (34)$$

where these new states reflect the new information contained in the latest measurements. This entire procedure is repeated until the specified end time.

2.7.2. Starting Requirements

Before the simulation process can begin, there are several input parameters which must be specified. This section lists these parameters, and also includes some typical ranges of values, in order to provide a more clear indication of the nature of the analysis. To begin, an initial nominal state (\mathbf{x}_0) must be specified, as well as an initial state covariance matrix (\mathbf{P}_0). The chaser was chosen to be trailing the target at the start of the simulation by nominally 50 km; in the homing phase, the chaser is to proceed on a trajectory to 2 km in front or behind the target (an input parameter), at which point the differential GPS processing will begin. \mathbf{P}_0 is assumed to be diagonal, with position and velocity standard deviations of 60 m and 1 m/s, respectively. Assuming that the chaser has been tracking GPS since orbit injection, the position knowledge should be around 30 m RSS; a worst case value of twice this was taken for this simulation. From this nominal initial state, values for the true and estimated states are determined by calculating two different error vectors consistent with \mathbf{P}_0 , and adding them to the nominal state.

In order to propagate the true state, the state noise covariance matrix (\mathbf{Q}_k) must be specified. This matrix is assumed to be diagonal, and to be a fraction of the drag force at the rendezvous altitude. The standard deviation of the diagonal terms is calculated by first determining the acceleration due to drag at the spacecraft altitude²¹

$$a_D = -\frac{\rho}{2} \left(\frac{C_D A}{m} \right) V^2 \quad (35)$$

where ρ is the density at altitude, and V is the velocity of the spacecraft. The reciprocal of the terms in the parenthesis is called the ballistic coefficient, and is an input parameter for the simulation. For this investigation a value of 90.9 kg/m^2 (18.6 lb/ft^2) is assumed; this is calculated using a mass of 200 kg , a cross sectional area of 1 m^2 , and a drag coefficient of 2.2 . This choice reflects the fact that the nature of the chaser is a small resupply or repair spacecraft. The above acceleration is integrated once over the specified Δt to obtain an "uncertainty velocity due to drag", and twice to obtain an "uncertainty position due to drag". These values are then used as the standard deviation of the position and velocity in the state noise matrix

$$\begin{aligned} \sigma_r &= -\frac{\rho}{2} \left(\frac{C_D A}{m} \right) V^2 \frac{\Delta t^2}{2} \cdot f_r \\ \sigma_v &= -\frac{\rho}{2} \left(\frac{C_D A}{m} \right) V^2 \Delta t \cdot f_v \end{aligned} \quad (36)$$

where f_r and f_v are scale factors, nominally set to 0.1 to represent typical errors in ρC_D . This procedure yields the state noise matrix for this simulation, and will serve to reflect uncertainties in modeling the system.

The last parameter which must be specified is the measurement noise. As was described in the above section, the measurement noise matrix must be expressed in terms of the pseudorange measurement errors. This is because these errors lie on the path between the receiver and the GPS satellite. The standard deviation of these pseudorange errors are assumed to be 27 m and 39 m for this study. As described previously, these errors are then transformed through the use of the \mathbf{A}^{-1} matrix for each particular measurement geometry.

2.7.3. Correlated Pseudorange Measurement Errors

An assumption in the Kalman filter is that the measurement errors are uncorrelated. This assumption places a restriction on the time permitted between pseudorange observations. More clearly, if pseudorange measurements are taken at one second intervals during the simulation, it is assumed that these would be correlated. Because a fundamental assumption is violated in this case, the filter will not be an unbiased, minimum variance, consistent estimator²². In order to avoid this problem, the time in between measurements is nominally set to three minutes (private communication, Kathy Thornton, Jet Propulsion Laboratory, September, 1993). Over this span of time,

the assumption is that the observations are not correlated, preserving the optimality of the Kalman filter.

2.7.4. Covariance Consistent, Random Vectors

One last point must be mentioned about the use of the Kalman filter. The method at various points requires the generation of error vectors consistent with a given covariance matrix. For example, state and measurement noise vectors must be generated such that they are consistent with the matrices \mathbf{Q}_k and \mathbf{R}_k , respectively. To generate such random vectors, an eigen-analysis is performed on the covariance matrix in question. The square roots of the eigenvalues (the standard deviations) are each multiplied by a different normally distributed random number. These products are then multiplied by the corresponding eigenvectors, and the resulting vectors are added to yield the statistically consistent random vector. This is expressed mathematically as

$$\mathbf{X}_{rand} = \begin{Bmatrix} x_1 \\ x_2 \\ \vdots \\ x_3 \end{Bmatrix} = \left\{ r_1 \sigma_1 \begin{Bmatrix} v_{11} \\ v_{21} \\ \vdots \\ v_{n1} \end{Bmatrix} + r_2 \sigma_2 \begin{Bmatrix} v_{12} \\ v_{22} \\ \vdots \\ v_{n2} \end{Bmatrix} + \dots + r_n \sigma_n \begin{Bmatrix} v_{1n} \\ v_{2n} \\ \vdots \\ v_{nn} \end{Bmatrix} \right\} \quad (37)$$

where σ_j are the square roots of the eigenvalues, r_j are normally distributed random numbers with mean zero and unity variance, and v_{jk} are the components of the eigenvectors.

2.8. Maneuvering Errors

In order to investigate possible control laws for the rendezvous maneuver, the capability of modeling spacecraft maneuvers must be incorporated in the simulation. This was described in Section 2.2.2, *Chaser Maneuvers*. In addition, the ability to simulate errors in these corrective burns has been included as well. The modeling of burn errors is performed through the use of two variables that account for magnitude and direction errors. As mentioned previously, magnitude errors could be due to burn time errors, specific impulse errors, and the like, whereas direction errors could be attributed to spacecraft attitude errors, thruster misalignment, or other effects. Specifically, the quantities chosen to model these burn errors are the standard deviations of the magnitude and direction of the burn as a percentage of the burn itself. Thus, as one would expect, with a larger ΔV , there will be associated a larger burn error. These variables are input parameters, so that a variety of configurations may be investigated.

For this research it is assumed that all maneuvers are instantaneous. This implies that the position and its covariance do not change during the maneuver, whereas the velocity and its covariance do change. The actual procedure to determine the new velocity values involves the following steps. The desired velocity, \mathbf{V}_{des} , is determined via the method described in 2.2.2, *Chaser Maneuvers*, and the nominal ΔV is calculated

$$\Delta \mathbf{V}_{nom} = \mathbf{V}_{old} - \mathbf{V}_{des} \quad (38)$$

The velocity *estimate* after the burn becomes this desired velocity, because lacking any other knowledge, the new velocity should on average be the nominal expected velocity

$$\hat{\mathbf{V}} = \mathbf{V}_{des} \quad (39)$$

Next, the corrupted *truth* velocity after the maneuver is calculated. As mentioned above, there are two parameters describing the $\Delta\mathbf{V}$ error. The first, σ_m , is the standard deviation of the magnitude of the corrective burn, given as a percent of nominal standard deviation. Thus, the component of the perturbed $\Delta\mathbf{V}$ vector along the nominal $\Delta\mathbf{V}$ axis is given by

$$\Delta V_1 = \|\Delta\mathbf{V}_{nom}\|(1 + r_1\sigma_m) \quad (40)$$

where r_1 is a normally distributed random variable with zero mean and unity variance. In this study, a value of 0.5% is utilized for the nominal σ_m .

The second parameter, σ_d , describes the direction deviation of the $\Delta\mathbf{V}$ vector from the nominal. It represents the standard deviation of the burn error along two orthogonal axis, each perpendicular to ΔV_1 . As described previously, the numerical value for σ_d is obtained from the RSS of two components. The first component accounts for thruster misalignment, and can be considered as a floor value for the direction error; this is nominally set at 0.01° . The second contribution is derived from the knowledge of the chaser's attitude (Section 5, *GPS Attitude Determination*). The square root of the trace of the attitude covariance matrix is taken as the angular measurement error. To convert this to a percent of nominal $\Delta\mathbf{V}$, use the relation

$$\sigma_{d_{attitude}} = \tan(\sqrt{\text{Trace}(\mathbf{P}_{attitude})}) \cdot 100 \quad (41)$$

Then the $\Delta\mathbf{V}$ components in the cross directions are determined from

$$\begin{aligned} \Delta V_2 &= \|\Delta\mathbf{V}_{nom}\|(r_2\sigma_d) \\ \Delta V_3 &= \|\Delta\mathbf{V}_{nom}\|(r_3\sigma_d) \end{aligned} \quad (42)$$

Thus, these three components form a perturbed $\Delta\mathbf{V}$ vector in a frame attached to the nominal $\Delta\mathbf{V}$ vector

$$\Delta\mathbf{V}_{\Delta V} = \|\Delta\mathbf{V}_{nom}\| \begin{Bmatrix} 1 + r_1\sigma_m \\ r_2\sigma_d \\ r_3\sigma_d \end{Bmatrix} \quad (43)$$

This vector represents the true velocity after the maneuver, expressed in a coordinate frame attached to the nominal velocity vector. All that remains is to convert this vector to

the target orbital frame, utilizing standard transformation procedures. Finally, the true velocity is found from the relation

$$\bar{\mathbf{V}} = \bar{\mathbf{V}}_{old} + \boldsymbol{\varphi}_{\Delta V \rightarrow tof} \Delta \mathbf{V}_{\Delta V} \quad (44)$$

where $\boldsymbol{\varphi}_{\Delta V \rightarrow tof}$ is the DCM from the "nominal velocity frame" to the target orbital frame. To summarize, the new velocity *estimate* after a corrective maneuver is the desired value of the velocity to arrive at the target in the specified time. The new *true* velocity is this desired value plus extra terms accounting for possible execution errors.

Along with an instantaneous change in the velocity vector, there must also be an instantaneous change in the velocity covariance. Knowing that the parameters σ_m and σ_d describe the burn errors in the nominal $\Delta \mathbf{V}$ frame, the covariance matrix in this frame is given by

$$\mathbf{P}_{\Delta V} = \begin{bmatrix} (\|\Delta \mathbf{V}_{nom}\| \sigma_m)^2 & 0 & 0 \\ 0 & (\|\Delta \mathbf{V}_{nom}\| \sigma_d)^2 & 0 \\ 0 & 0 & (\|\Delta \mathbf{V}_{nom}\| \sigma_d)^2 \end{bmatrix} \quad (45)$$

The conversion of this covariance to the target orbital frame is carried out through the use of the covariance propagation law

$$\mathbf{P}_{tof} = \boldsymbol{\varphi}_{\Delta V \rightarrow tof} \mathbf{P}_{\Delta V} \boldsymbol{\varphi}_{\Delta V \rightarrow tof}^T \quad (46)$$

Finally, the velocity covariance after a corrective maneuver is given by adding this new contribution to the old value

$$\mathbf{P}_{new} = \mathbf{P}_{old} + \mathbf{P}_{tof} \quad (47)$$

2.9. Pseudorange Results

2.9.1. Simulation Integrity

Before proceeding to the full scale analysis, it was desired to investigate some of the fundamental outputs to validate the simulation. Several types of data were examined, all of which were verified through intuitive analyses. This was performed simply to achieve order of magnitude agreement. Shown below are the results from two such investigations. It is expected that a smaller GPS constellation will yield fewer SVs in sight at any given time; this obvious result is verified in Figure 2.9.1.a. Also, the imposition of an elevation angle implies that fewer SVs will be in sight, as shown in Figure 2.9.1.b.

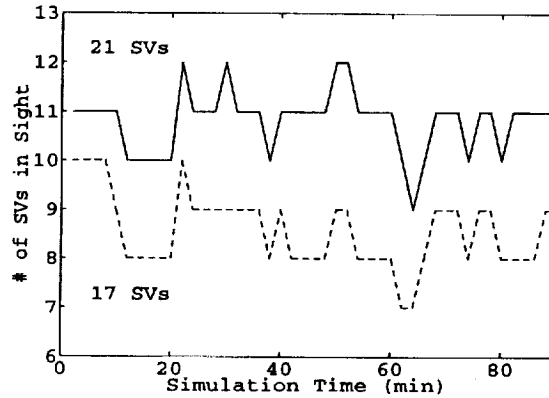


Figure 2.9.1.a: Effect of Constellation Size on SV Observability

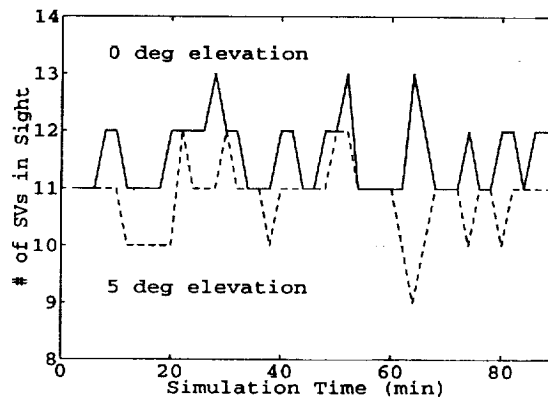


Figure 2.9.1.b: Effect of Elevation Angle on SV Observability

2.9.2. Position Knowledge and Monte Carlo Verification

For linear problems, Kalman filters produce exact results that, if programmed correctly, do not require verification. However, some procedures in this analysis are nonlinear, so there is a question as to the validity of a linear covariance analysis. As a result, it was desired to utilize a Monte Carlo analysis to examine the performance of this simulation. Table 2.9.2.a shows the results of four Monte Carlo simulations with 500 runs each, and their corresponding error analyses. The first column is the standard deviation of the measurement noise for the simulations. The remaining two columns represent the true position errors as determined from the Monte Carlo simulation, and the knowledge of the position errors calculated from the error analysis, both at the end of the homing phase.

Table 2.9.2.a: Monte Carlo Verification of Position

	1σ Noise (m)	Monte Carlo (m)	Error Analysis (m)
No SA	15.0	9.7	10.7
Gaussian SA	27.0	17.1	18.3
SA via Braasch Model	27.0	21.6	19.1
SA via Braasch Model	38.3	28.2	26.4

The first case, no SA, represents when the intentional degradation of the GPS signal is not activated, and typical measurement errors are assumed to be normally distributed with a standard deviation of 15 m. The second case, Gaussian SA, is a test case in which the SA is active, and is assumed to be normally distributed with a standard deviation of 27 m. The remaining two rows assume SA is activated and consistent with the Braasch model, with measurement noise levels of 27.0 and 38.3 m.

The table shows that for the no SA and Gaussian SA cases, the Monte Carlo and error analysis statistics are consistent as expected; these two cases serve to verify the use and operation of the linear filter. In addition, the cases involving SA residuals derived from real data are also statistically consistent, implying that the assumptions in this research (particularly the measurement time interval of 3 minutes) are proper. Thus, the Kalman filter can be utilized to estimate the chaser state, even in the presence of intentional degradation of the GPS signal.

2.9.3. Homing Phase State Knowledge, SA Active

Before presenting the results of this analysis, a brief explanation is in order about the presentation of the simulation results in this and the remaining sections of the paper. In most cases, results are desired comparing the receiver knowledge of the state to the actual state errors. As a result, in most figures, two sets of data are plotted. First, the standard deviation calculated in the error analysis is plotted using *solid* lines; this represents the state knowledge. Second, the residual, or the true value minus the estimate, is plotted using *dashed* lines. Also, in figures showing the position and velocity, the three components of each are all shown. If all the assumptions in the simulation are correct, the error analysis results represent the average of an infinite number of simulation residuals. Thus, it can be expected that the error analysis and each particular instance of simulation residuals will be consistent. For example, consider the rendezvous case with corrective burns at 15 and 84 minutes, and assume SA noise levels of 27 m; the time histories of position and velocity knowledge are shown in the figures below. In Figure 2.9.3.a, the position knowledge (three solid lines) and the position residual (three dashed lines) remain consistent, displaying the same trend. This is the case in the velocity knowledge as well, shown in Figure 2.9.3.b. Hence, the simulation is statistically consistent, and the Kalman filter can be used to estimate the state in the homing phase of an automated rendezvous. For SA noise levels of 27 m, position knowledge is maintained on the order of 20 m, and velocity on the order of $2 \cdot 10^{-2}$ m/s (RSS), and for SA noise of 39 m, 27 m position and $4 \cdot 10^{-2}$ m/s velocity RSS knowledge is achievable.

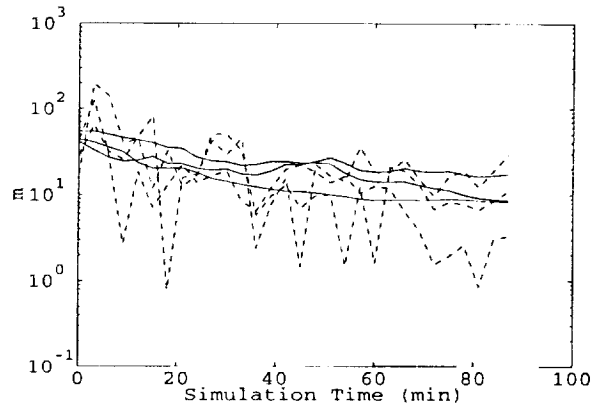


Figure 2.9.3.a: Homing Phase Position Knowledge and Residual

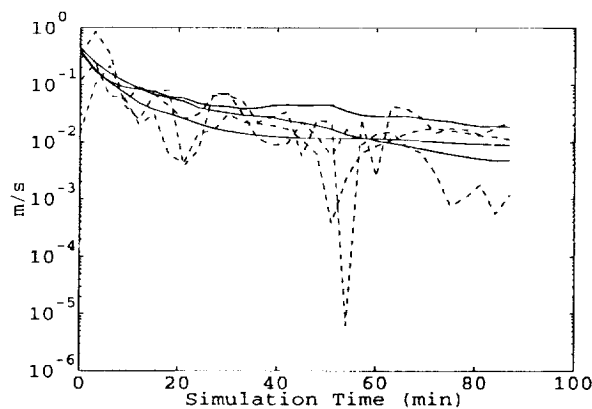


Figure 2.9.3.b: Homing Phase Velocity Knowledge and Residual

2.9.4. Guidance Strategies

When evaluating guidance strategies for the homing phase, the final solution will be a compromise between two conflicting requirements. First, as little fuel as possible (within requirements) should be utilized, and second, the deviation between nominal and true final positions should meet the prescribed requirements. It might be argued that the second requirement is not critical, because no matter how poor the guidance is during the homing phase, good control during the stationkeeping and terminal phases will result in a satisfactory rendezvous. However, the flaw in this argument involves the possibility of collision. Because the two spacecraft are in such close proximity at the end of the homing phase (2 km), significant maneuvering error could lead to mission failure. As a result, maneuvering errors must be sufficiently small that the probability of collision is within prescribed limits.

Several simulations with SA noise levels of 27 m were performed to generate an example of these concepts. The results are shown in Figure 2.9.4.a, where exaggerated system errors were used to illustrate the effects more clearly. It is a plot of the ΔV requirement and the corresponding control errors for varying maneuver times. The propellant requirement is expressed as the "statistical ΔV ", calculated from the relation

$$\Delta V_{\text{statistical}} = \Delta V_{\mu} + \Delta V_{3\sigma} - \Delta V_{\text{nominal}} \quad (48)$$

where $\Delta V_{\mu} + \Delta V_{3\sigma}$ is the mean plus 3σ value of the ΔV , calculated from Monte Carlo simulations, and $\Delta V_{\text{nominal}}$ is the ΔV requirement along the nominal trajectory, in the absence of any errors. For the case of the chaser trailing the target by 50 km, the nominal ΔV requirement is 6.03 m/s. The statistical ΔV represents the excess fuel required above the nominal to account for 3σ errors. The control errors are deviations in the final position of the spacecraft due to errors in maneuvering.

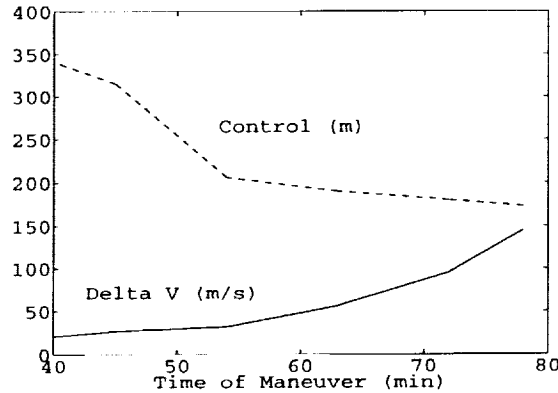


Figure 2.9.4.a: Exaggerated One Burn ΔV Requirements and Control Errors

Several facts can be gathered from this figure. Early maneuvers require smaller ΔV 's; however, poorer state knowledge at this earlier time (due to fewer measurements) leads to execution errors. In addition, errors in an early maneuver map into larger errors. On the other hand, if the maneuver is performed later, the ΔV requirement increases as the chaser approaches the target. There are advantages to a late maneuver, however, one being that because the state knowledge has improved (due to more measurements), the burn is less likely to be incorrect. Also, a late maneuver implies that any ΔV error will not have the time to propagate into significant control errors.

It is evident from this analysis that one maneuver is not sufficient to achieve both minimum fuel and minimum control error. As a result, several combinations of two corrective maneuvers have been investigated. A maximum of two maneuvers was utilized in order to maintain a relatively low mission complexity. A good compromise seems to be achieved when there is a burn shortly after the homing phase initiation, and a burn shortly before the end of the homing phase. This makes intuitive sense based on the following argument. Because the state knowledge at the start of the simulation is poor, the initial burn, ΔV_1 , is in error. After only a few minutes of tracking, the state knowledge is improved, so the majority of the control errors of ΔV_1 can be eliminated by a first corrective burn, ΔV_{2a} . An added benefit is that this early burn has a lower propellant requirement. Then, with the chaser much closer to the nominal trajectory, a maneuver near the final time (ΔV_{2b}) is used to ensure that the control errors are within the desired limits.

The tables below show the results of the investigation into the use of several possible two maneuver combinations, assuming SA noise levels of 27 m. Table 2.9.4.a investigates varying first corrective maneuver times (ΔV_{2a}), and Table 2.9.4.b varying second corrective maneuver times (ΔV_{2b}). Both tables include a ΔV analysis and a final position analysis. As described above, the "statistical ΔV " is used as the performance index for the ΔV analysis. For the control analysis, the concept of the b-plane is used. The b-plane is an imaginary plane perpendicular to the nominal trajectory at the desired end time (the end of the homing phase). Thus, any chaser position errors *perpendicular* to the b-plane are time of arrival errors, and do not contribute to a miss of the desired terminal point. However, errors *in* the b-plane do represent rendezvous trajectory errors. Therefore, the parameter used for the control analysis is the RSS of the position errors in the b-plane at the rendezvous time; this measure describes how far the chaser is likely to miss the desired end point.

Table 2.9.4.a shows the effects of varying the first corrective maneuver time, while keeping the final burn time fixed at 81 minutes. For this investigation, the total homing phase time is 90 minutes. There is a minimum ΔV requirement at a first burn time around 15-21 minutes. Note that, because the final burn time is fixed, this establishes the control errors at the homing phase end to around 30 m for all cases, so this is not a factor in these results.

Table 2.9.4.a: Homing Phase Two Burn Combinations: First Burn Times

Burn Times	ΔV Analysis (m/s)			B-Plane Control (m)	
	Mean	1σ	$\Delta V_0 + \Delta V_{3\sigma} - \Delta V_{nom}$	Mean	1σ
12, 81 min	13.0	4.35	20.0	3.16	29.1
15, 81 min	11.2	3.03	14.3	1.93	30.0
21, 81 min	11.1	3.08	14.3	1.58	29.7
30, 81 min	11.1	3.58	15.8	0.847	34.7
39, 81 min	13.1	4.89	21.7	2.79	29.8
45, 81 min	15.0	6.58	28.3	2.74	29.6
54, 81 min	18.2	9.72	41.3	4.25	29.2

It is also desired to investigate varying the final burn time while keeping the initial maneuver time fixed. The initial burn time was chosen to be 15 minutes based on the results of Table 2.9.4.a. The results, shown in Table 2.9.4.b, indicate that there is a minimum ΔV requirement at a second burn time of 72 minutes. However, unlike above, the control plays an important role in this analysis, because the time for minimum maneuver requirement does not correspond to the time for minimum final control. A typical tradeoff is evident; the final decision depends on whether minimum propellant mass or minimum control error is more critical. A reasonable compromise is reached if the first corrective maneuver is performed in the neighborhood of 15-20 minutes, and the second around 75-85 minutes. Given a more well defined system, including a cost function involving velocity increments (ΔV) and control errors (σ), optimization methods

could be utilized to determine the minimum propellant and minimum control solutions subject to the system constraints.

Table 2.9.4.b: Homing Phase Two Burn Combinations: Second Burn Times

Burn Times	ΔV Analysis (m/s)			B-Plane Control (m)	
	Mean	1σ	$\Delta V_0 + \Delta V_{3\sigma} - \Delta V_{nom}$	Mean	1σ
15, 87 min	16.1	7.14	31.48	3.64	23.0
15, 84 min	12.9	4.46	20.3	5.68	26.1
15, 78 min	10.2	2.35	11.2	2.11	40.9
15, 72 min	9.37	2.06	9.52	1.31	49.3
15, 63 min	9.41	2.25	10.13	3.89	76.7

2.9.5. Effects of Modeling SA Measurement Noise Incorrectly

For all of the above analyses, the measurement noise statistics were assumed to be consistent with the noise levels due to SA. In other words, if the actual standard deviation of the SA residual data was 27 m, the measurement noise was also set to this level. However, it may not always be possible to estimate the SA noise accurately; as a result, it was desired to investigate errors in modeling this parameter. To accomplish this, the true SA noise level was fixed at 27 m, and the filter measurement noise was varied from 7 m to 47 m. The results are shown in Table 2.9.5.a, which shows both the Monte Carlo final position standard deviation and the error analysis position knowledge as a function of the assumed measurement noise levels. As discussed in Section 2.9.2, *Position Knowledge and Monte Carlo Verification*, when the true and filter statistics are the same (27 m), the Monte Carlo and error analysis results are consistent. In addition, because the true noise levels on all the simulations are the same (27 m), the Monte Carlo results are all on the same level (~ 20 m). On the other hand, as the assumed measurement noise is varied, the error analysis values change directly; if the SA measurement noise is too low, then the state errors are underestimated, and if the SA noise is too high, then the errors are overestimated. For example, if the SA measurement noise is assumed to be 7 m, then the error analysis will imply that the position is known to within 5.3 m, when in actuality, true errors are on the order of 21 m. This is undesirable because unknown errors lead directly to an increase in mission risk. On the other hand, if the SA noise is to be 47 m, then the error analysis will yield position knowledge of 29.8 m, when the true errors are actually much lower. As a result, the correct SA noise level must be utilized if the state knowledge is to be consistent with true errors; unfortunately, the nature of the SA noise level is never known ahead of time. One possible solution may be to deliberately overestimate typical SA noise levels; by doing so, the chances of underestimating the position errors is reduced.

Table 2.9.5.a: SA Measurement Noise Analysis

Assumed Measurement Noise (m)	Monte Carlo (m)	Error Analysis (m)
7	21.4	5.3
17	19.7	11.0
27	21.6	19.1
37	19.8	23.7
47	19.3	29.8

2.10. Homing Phase Conclusions

This portion of the investigation has brought to light several facets of utilizing GPS for the homing phase of an automated rendezvous mission. First, the use and operation of the Kalman filter was verified. Test cases assuming Gaussian SA noise were shown to be statistically consistent, as were cases utilizing modeled SA noise. Second, in the presence of 27 m SA noise, the Kalman filter was shown to yield position knowledge in the homing phase on the order of 20 m RSS, and velocity knowledge on the order of $2 \cdot 10^{-2}$ m/s RSS. When 39 m SA noise is assumed, the position and velocity knowledge approaches 27 m and $4 \cdot 10^{-2}$ m/s RSS, respectively. In later sections, it will be shown that the stationkeeping mode requires only about 10 minutes, so during this time period, the residual velocity maps into a displacement of only about 15-30 m. Third, guidance strategies involving one and two corrective maneuvers were investigated. It was found that a corrective maneuver performed shortly after the homing phase initiation (~15 minutes) eliminates much of the error in the initial burn, and requires lower levels of propellant than a later maneuver. A second maneuver shortly before the end of the homing phase (~10 minutes) ensures that the final control errors will be on the order of 30 m. Finally, the mismodeling of SA error statistics was shown to lead to inconsistencies in the statistical output of the simulation; overestimation of this parameter may be advisable to reduce mission risk.

3. Stationkeeping via Differential GPS

3.1. Overview

Section 2, *Position Determination from Pseudorange Measurements*, described the homing phase of the automated rendezvous. During this section of the mission, it was only desired to maintain a coarse estimate of the chaser's state, and the analysis showed that position and velocity knowledge of around 20 m and $2 \cdot 10^{-2}$ RSS, respectively, could be achieved. Once the chaser reaches about 2 km from the target, a maneuver is performed to enter a stationkeeping mode. As with all of the ΔV maneuvers, errors in the burn were modeled as described in Section 2.8, *Maneuvering Errors*. As a result, the chaser does not make a perfect burn to begin stationkeeping, and there remains some relative motion between the two spacecraft during this phase.

At the outset of the stationkeeping phase, the two spacecraft switch to differential GPS using the carrier phase observable to obtain higher accuracy *relative* positioning; pseudorange data is no longer processed. As described previously, when using carrier phase positioning, the initial integer ambiguity must be resolved before the phase information is of any value. This explains the need for the chaser to establish a quasi-constant distance from the target: to resolve the integer ambiguities. If, rather than entering a stationkeeping mode, the chaser attempts to resolve the integer ambiguities while on a trajectory to rendezvous with the chaser, there is a significant chance that the ambiguities will not be determined before the rendezvous time. Without the accurate phase data, the chaser will have to rely on the coarse pseudorange data, whereupon the risk of mission failure is greatly increased. Thus, the chaser must maintain a quasi-constant distance while the GPS carrier is tracked. Filtering the phase measurements, as described below, should resolve the unknowns, so that continuous carrier phase tracking can be used in the terminal phase of the rendezvous.

3.2. Differential GPS and the Integer Ambiguity

This entire development of differential GPS and resolving the integer ambiguities on the fly is based on the discussion in Hwang²³. When utilizing GPS carrier phase measurements to determine relative positions, the periodic nature of the signal introduces an ambiguity which must be resolved before the entire solution can be determined. Consider Figure 3.2.1.a, which is an example of a single one dimensional static phase measurement situation.

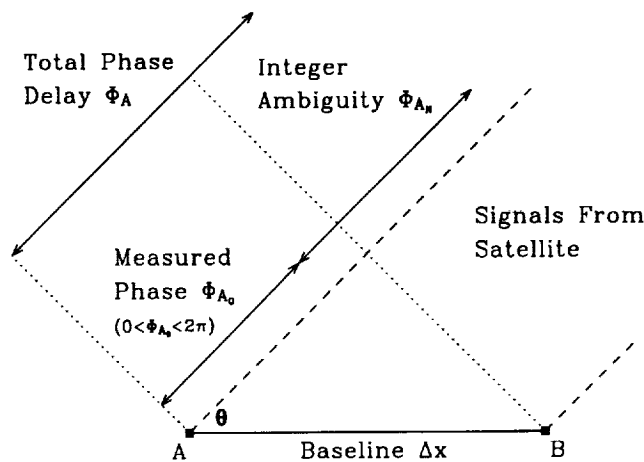


Figure 3.2.1.a. One Dimensional Static Phase Measurement²⁴

The phase difference between points A and B is utilized for the relative positioning. The total phase difference is calculated from

$$\Delta\phi = \phi_A - \phi_B = \cos\theta \cdot \Delta x \quad (49)$$

This measurement is composed of a part due to the number of whole phase cycles, $\Delta\phi_N$, and a part due to the measured phase difference, $\Delta\phi_0$, so that

$$\Delta\phi = \Delta\phi_0 + \Delta\phi_N = \cos\theta \cdot \Delta x \quad (50)$$

The whole cycle count, $\Delta\phi_N$, is unknown at the start of the tracking and is called the initial integer ambiguity. Thus, the measured phase difference is

$$\Delta\phi_0 = \cos\theta \cdot \Delta x - \Delta\phi_N \quad (51)$$

Only after this ambiguity has been determined does the continuous tracking of the carrier signal yield complete knowledge of the relative position of the two receivers.

It is important to mention that while the above discussion was based on a simple single phase difference measurement, in actuality there is a problem associated with this type of measurement in the form of the clock error. The true phase difference is given by

$$\Delta\phi_0 = \cos\theta \cdot \Delta x - \Delta\phi_N + \omega\Delta t \quad (52)$$

where the clock error Δt is due to the time difference in the receiver clocks at A and B. To eliminate the clock offset, the phase difference from two different satellites is subtracted, forming the double difference measurement. The critical assumption is that the measurements are taken simultaneously. Given the following two single difference measurements, where the parenthetical superscript denotes the SV,

$$\begin{aligned} \Delta\phi_0^{(1)} &= \cos\theta^{(1)} \cdot \Delta x - \Delta\phi_N^{(1)} + \omega\Delta t \\ \Delta\phi_0^{(2)} &= \cos\theta^{(2)} \cdot \Delta x - \Delta\phi_N^{(2)} + \omega\Delta t \end{aligned} \quad (53)$$

the following double difference is formed

$$\Delta\phi_0^{(1)} - \Delta\phi_0^{(2)} = (\cos\theta^{(1)} - \cos\theta^{(2)}) \cdot \Delta x + (\Delta\phi_N^{(2)} - \Delta\phi_N^{(1)}) \quad (54)$$

where the clock offset is seen to cancel. Thus, the measurements used in the simulation are the double differences, and the unknown ambiguities are actually the differences of two large integers.

Determining the initial integer ambiguities (actually integer difference ambiguities) can be accomplished on the ground typically through three methods. First, the ambiguities could be initialized by calibrating the receivers with a known baseline; this method provides an instantaneous solution. Second, the antenna swap method could be used, in which the receivers exchange positions to resolve the unknowns²⁵. Third, a static survey could be performed, which would provide a known baseline for future surveys. Unfortunately, none of these methods are applicable to the orbital rendezvous problem.

One way to determine the integer ambiguities on-orbit is through the use of some type of filtering procedure. There are two main families of filters that could be used,

either batch or sequential (the Kalman filter, for this investigation). Noting that the homing, terminal, and attitude sections of this study all utilize the Kalman filter (because the batch filter is not appropriate for those cases), the same filter was chosen for use in the stationkeeping phase, for the ease of implementation. The main disadvantage of this approach is that values that are known to be integers are estimated as continuous random variables. At the time of this writing, the author was aware of only one investigation into the use of a sequential filter that takes advantage of the knowledge that these ambiguities are integers²⁶. It is possible to utilize a parallel bank of Kalman filters, with each corresponding to an integer ambiguity assumption. The filter that corresponds to the correct solution converges to 1, while the others converge to 0. A drawback to this method is its large computational requirement. For example, real life position uncertainty values may be on the order of a few meters, which corresponds to an integer ambiguity uncertainty of 100 units in each of three dimensions. The utilization of this method for this case would require 100^3 or a million parallel filters. At this time, this type of computational requirement precludes the possibility of using this approach in practice. Thus, a standard Kalman filtering procedure is utilized, as described in the section below.

It should be noted that the batch filter does possess a particular advantage only for the area of resolving integer ambiguities in the stationkeeping mode. If a batch filter were used, the chaser would take measurements for some specified time, and then would process the entire bank of data, perhaps using a least squares method. The advantage of this type of method is that it is easier to utilize the fact that the ambiguities are integers. For example, if the least squares analyses yielded non integers for the ambiguities, then all possible combinations of integers bounding these values could be investigated. The one that provided the minimum residual would be chosen as the solution. The implementation of a batch filter for resolving the integer ambiguities in the stationkeeping mode requires further study.

3.3. Kinematic on the Fly GPS and Kalman Filtering

The idea behind the use of Kinematic on the Fly GPS is basically to utilize a Kalman filter to estimate not only the receiver position, but also the initial integer ambiguities from the phase double differences²⁷. There are two issues that must be discussed when utilizing this method. First, Kinematic on the Fly GPS should not be utilized to resolve the integer ambiguities while on a trajectory to rendezvous with the chaser (i.e., in the terminal phase); to do so may result in catastrophic failure. If the unknowns cannot be determined, then accurate phase position knowledge is not available, and only C/A pseudorange data can be used. Large position uncertainty (on the order of C/A errors) near rendezvous could result in target-chaser collision. As a result, the concept of the stationkeeping phase is utilized; about 2 km from rendezvous, a maneuver places the chaser in a quasi-stationary position relative to the target. Phase measurements are processed until the ambiguities are resolved and the relative state is fully known. At this point, high accuracy differential phase positioning can be used for the terminal phase of the rendezvous.

Second, the observability of the systems in question must be investigated. Consider the case where there is no knowledge of the trajectory of the receivers, as in Hwang²⁸. In this instance, there must eventually be enough measurements to solve for all

of the unknowns over the time period of interest. For example, consider the case of tracking seven satellites (from which six independent double differences can be formed at a time), and consider an interest only in the position and the integer ambiguities, and not the velocity. For one epoch, or time of measurement, there are three positions and six integer difference ambiguities, for a total of nine unknowns. Six measurements cannot fully describe these unknowns. However, for two epochs (t_0 and $t_0+\Delta t$), there are twelve measurements, and there are also twelve unknowns: three original positions at t_0 , three positions at $t_0+\Delta t$, and the same six integer ambiguities. Hence, the seven satellite case is a well posed problem for position and integer ambiguity knowledge over two epochs. Similarly, there are six and five satellite models for these conditions that are both well posed; however, the number of epochs required increases above the two needed for the seven satellite case. This translates directly into slower filter convergence. On the other hand, utilizing larger numbers of SVs becomes impractical because the probability of maintaining more than seven in view is reduced. The above discussion can be visualized more clearly by inspecting Table 3.3.1.a.

Table 3.3.1.a: Satellite Models and Their Observability, Estimating Position and Integer Ambiguity Only

<u># of SVs</u>	<u>Epoch #</u>	<u># of Msmts.</u>	<u># of Unknowns</u>
5	1	4	9
	2	8	12
	3	12	15
	4	16	18
	5	20	21
	6	24	24
6	1	5	9
	2	10	12
	3	15	15
7	1	6	9
	2	12	12

For the case of the orbital rendezvous, it is not sufficient to estimate the position and integer ambiguities; the velocity must be known as well. This adds three extra unknowns at every epoch, so that seven satellites will never be able to sufficiently determine the unknowns, no matter how many epochs are used. However, it is still possible to utilize the seven satellite model; the key lies in exploiting the information inherent in the system dynamics. The assumption of not knowing the trajectory of the receiver is valid in most cases; for example, if a GPS receiver were installed on a car or an aircraft, the dynamics would be controlled solely by the pilot, and hence could not be modeled for use in a Kalman filter. However, in the case of satellites in orbit, the trajectories are well known and can be quantified in the state transition matrix of the filter. Hence, it is possible that this added knowledge will allow the filter to estimate a

system with more unknowns than measurements. Based on the developments in the section above, the carrier phase observation matrix for the seven satellite case is

$$\begin{Bmatrix} \Delta\phi^{(1)} - \Delta\phi^{(2)} \\ \Delta\phi^{(2)} - \Delta\phi^{(3)} \\ \Delta\phi^{(3)} - \Delta\phi^{(4)} \\ \Delta\phi^{(4)} - \Delta\phi^{(5)} \\ \Delta\phi^{(5)} - \Delta\phi^{(6)} \\ \Delta\phi^{(6)} - \Delta\phi^{(7)} \end{Bmatrix} = \begin{bmatrix} h_x^{(1)} - h_x^{(2)} & h_y^{(1)} - h_y^{(2)} & h_z^{(1)} - h_z^{(2)} & 0 & 0 & 0 & 1 & 0 & 0 & 0 & 0 & 0 \\ h_x^{(2)} - h_x^{(3)} & h_y^{(2)} - h_y^{(3)} & h_z^{(2)} - h_z^{(3)} & 0 & 0 & 0 & 0 & 1 & 0 & 0 & 0 & 0 \\ h_x^{(3)} - h_x^{(4)} & h_y^{(3)} - h_y^{(4)} & h_z^{(3)} - h_z^{(4)} & 0 & 0 & 0 & 0 & 0 & 1 & 0 & 0 & 0 \\ h_x^{(4)} - h_x^{(5)} & h_y^{(4)} - h_y^{(5)} & h_z^{(4)} - h_z^{(5)} & 0 & 0 & 0 & 0 & 0 & 0 & 1 & 0 & 0 \\ h_x^{(5)} - h_x^{(6)} & h_y^{(5)} - h_y^{(6)} & h_z^{(5)} - h_z^{(6)} & 0 & 0 & 0 & 0 & 0 & 0 & 0 & 1 & 0 \\ h_x^{(6)} - h_x^{(7)} & h_y^{(6)} - h_y^{(7)} & h_z^{(6)} - h_z^{(7)} & 0 & 0 & 0 & 0 & 0 & 0 & 0 & 0 & 1 \end{bmatrix} \begin{Bmatrix} x \\ y \\ z \\ \dot{x} \\ \dot{y} \\ \dot{z} \\ N^{(1,2)} \\ N^{(2,3)} \\ N^{(3,4)} \\ N^{(4,5)} \\ N^{(5,6)} \\ N^{(6,7)} \end{Bmatrix} \quad (55)$$

where the parenthetical superscript refers to the GPS satellite, \mathbf{h} is the unit vector to the SV, (x, y, z) is the receiver position, $(\dot{x}, \dot{y}, \dot{z})$ is the receiver velocity, and $N^{(i,j)}$ is the integer ambiguity difference between the i^{th} and j^{th} SVs. The methods for utilizing this in propagating the Kalman filter are the same as in Section 2.7, *The Kalman Filter*.

3.3.1. Starting Requirements

At the end of the homing phase, the position, velocity, and the associated covariances remain the same; the integer ambiguity and an initial value for its covariance must be established. The true initial integer ambiguity difference is calculated from the true state ($\bar{\mathbf{r}}$) and the positions of the two SVs in question (ρ_i, ρ_j)

$$N^{(i,j)} = \text{fix}\left[\left(\|\rho_i - \bar{\mathbf{r}}\| - \|\rho_j - \bar{\mathbf{r}}\|\right) / \lambda\right] \quad (56)$$

where $\text{fix}()$ is the function that rounds the argument towards zero, and λ is the wavelength of the GPS carrier. The initial estimate of the integer ambiguity is calculated from this same formula, but replacing the state estimate ($\hat{\mathbf{r}}$) for the true state.

The integer ambiguity covariance matrix is calculated from the position knowledge at the end of the homing phase. If the position is known from the homing phase to σ_x , σ_y , and σ_z , then this establishes the appropriate range for the integer ambiguity uncertainty as well, due to their relation through the carrier wavelength. The trace of the covariance matrix is used because this will yield a conservative value. Also, since the integers to be estimated are actually integer differences, the range of the uncertainty is increased by a factor of $\sqrt{2}$. Thus, the integer ambiguity standard deviation is given by

$$\sigma_N = \frac{1}{\lambda} \sqrt{2 \cdot \text{Trace}(\mathbf{P}_{xyz})} \quad (57)$$

The state noise for the positions and velocities were computed the same way as in the homing phase. As described in Section 2.7.2, 10% of the acceleration due to drag at the rendezvous altitude was used. The integer ambiguity state noise was determined from the position state noise using the factor $\sqrt{2} / \lambda$, as above.

The measurement noise for the phase double differences is determined first by establishing the knowledge on a single phase measurement. This study investigates two different knowledge levels on this measurement, 15° and 5°; this will provide an idea of the measurement accuracy required. The 15° level is the worst case phase knowledge measured in a ground test of single difference GPS attitude determination²⁹, and 5° is used as a more optimistic estimate. Because the actual measurement used in the filter is a double difference, a factor of $\sqrt{2} \cdot \sqrt{2} = 2$ is utilized to account for the differencing process. For example, if it is assumed that the measurement noise level is 15°, then the double difference noise will be on the order of 30°.

3.3.2. Correlated Phase Measurement Errors

As discussed in Section 2.7.3, *Correlated Pseudorange Measurement Errors*, an assumption in the Kalman filter is that the measurement noise is uncorrelated. As with the pseudorange, the phase sampling rate cannot be so high that the measurement noise becomes correlated. A phase sampling interval of two seconds has been suggested in prior discussions³⁰, so this is the value used in the current investigation.

3.4. GPS Satellite Tracking

At the start of the stationkeeping phase, it is necessary to select seven satellites for use in the resolution of the integer ambiguities. This is accomplished by propagating the satellite orbits and the receiver orbits, and determining line of sight for all the SVs until they drop out of view. In this simulation, this is an easy task because the orbits are already calculated and stored in tables. In a real mission, this is a solvable problem as well, because all satellite orbits are predictable. The seven satellites are then selected simply by choosing those that will stay in view the longest.

There is the question of whether or not these seven satellites will stay in view for the entire process of resolving the integer ambiguities. In this simulation, the resolution process took on average about 10 minutes, and it was possible to maintain seven satellites in view for this period of time. If, however, a satellite were to drop out of view before the integers were resolved, the solution would be to start the integer resolution process over again with seven new satellites and resolve the new ambiguities. With the optimal 21 satellite constellation in place, it will not take long for an acceptable set of satellites to come into view. This solution is plausible for all the missions this investigation is concerned with, because the delay of a few orbits will have no significant impact on accomplishing the mission objectives. As mentioned previously, the velocity uncertainty in the chaser ($2 \cdot 10^{-2}$ m/s) is not critical; even if the resolution process takes an hour, this

velocity maps into a displacement of less than 100 m. The chaser will still be far enough from the target to ensure safety, while not imposing restrictive ΔV requirements.

3.5. Stationkeeping Results

3.5.1. State Knowledge: 15° Measurement Noise

Figures 3.5.1.a-c show the knowledge of the position, velocity, and ambiguities for a standard stationkeeping phase, assuming 15° measurement noise. In each case, the advantages of differential GPS are shown; the knowledge benefits are two orders of magnitude or more over standard C/A positioning. The position knowledge decreases from around 20 m to 0.03 m, the velocity from $2 \cdot 10^{-2}$ m/s to $2 \cdot 10^{-5}$ m/s, and the ambiguities from 30 wavelengths to 0.2 wavelengths.

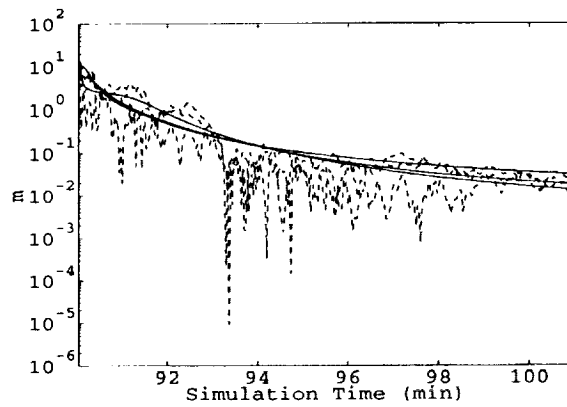


Figure 3.5.1.a: Stationkeeping Position Knowledge and Residual, 15° Measurement Noise

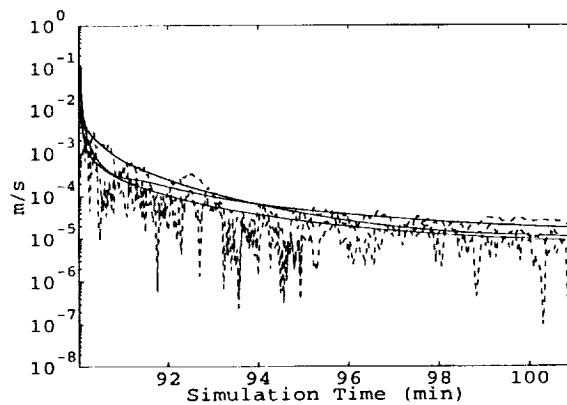


Figure 3.5.1.b: Stationkeeping Velocity Knowledge and Residual, 15° Measurement Noise

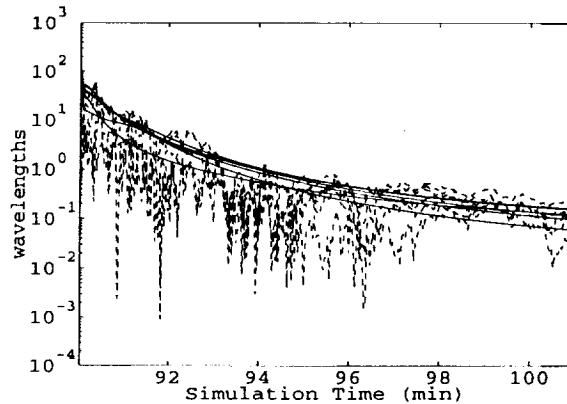


Figure 3.5.1.c: Stationkeeping Ambiguity Knowledge and Residual, 15° Measurement Noise

An interesting point to note is that while a static survey on the ground (no receiver motion) typically requires 20-30 minutes to completely resolve the integer ambiguities, the kinematic method for the satellites in orbit only requires about 10 minutes. This may be due to the observability of the systems in question. For the static initialization, the resolution of the ambiguities is almost completely dependent on the motion of the GPS satellites to create a sufficiently observable system. However, for the case of the satellites in orbit, the position of the receiver is changing much more rapidly, possibly resulting in increased observability of the SVs, and hence a faster convergence time.

Another result to notice is that the ambiguities are resolved in the orbital case in less than half the time than a ground use of Kinematic on the Fly³¹. Most likely, this is due to the fact that the mechanics of the system are exploited in the rendezvous. If the state is simply allowed to random walk, then there is no knowledge of the relation between the states at one epoch and the next. However, the mechanics in the rendezvous are well known and thus can be used to enhance the knowledge of the state. The overall effect, then, is to provide faster solution convergence.

3.5.2. State Knowledge: 5° Measurement Noise

The results of using more accurate measurements is shown in Figures 3.5.2.a-c. One result is clear: the state knowledge converges at a faster rate. Whereas the above poorer measurement case required approximately 10 minutes to converge, this case only requires about 7 minutes. This observation is purely academic. Because the chaser can generally remain in stationkeeping mode until the ambiguities are known, the time to convergence is not an important factor here.

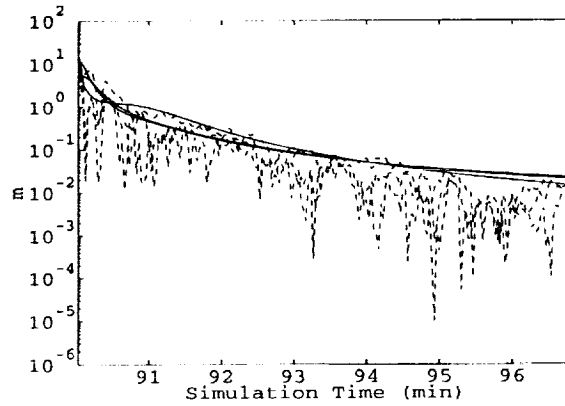


Figure 3.5.2.a: Stationkeeping Position Knowledge and Residual, 5° Measurement Noise

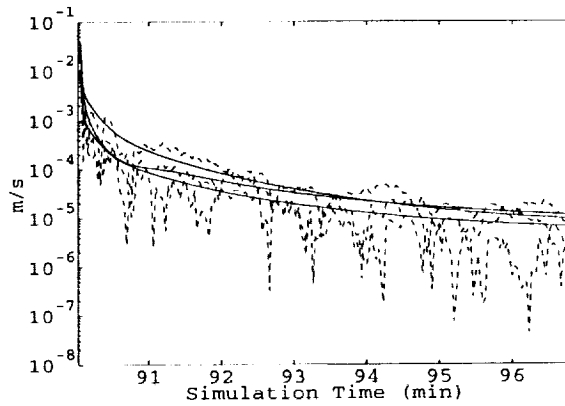


Figure 3.5.2.b: Stationkeeping Velocity Knowledge and Residual, 5° Measurement Noise

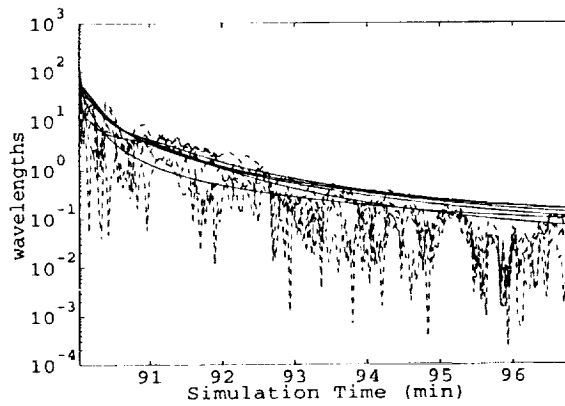


Figure 3.5.2.c: Stationkeeping Ambiguity Knowledge and Residual, 5° Measurement Noise

3.5.3. GPS Satellite Usage: 3, 5, and 7 SVs

The results in the above sections were obtained through the use of 7 GPS satellites. However, as described in Section 3.3, *Kinematic on the Fly GPS and Kalman Filtering*, it may not be necessary to utilize this full set. Because the system dynamics are known, this added knowledge may make it possible to achieve comparable accuracies while using fewer SVs. Note that by tracking fewer satellites, fewer ambiguities need to be estimated in the Kalman filter. For this part of the investigation, it is assumed that the measurement noise is 5° . Figures 3.5.3.a-c show that it is indeed possible to utilize only 5 satellites while still achieving results on the same order as the 7 satellite case.

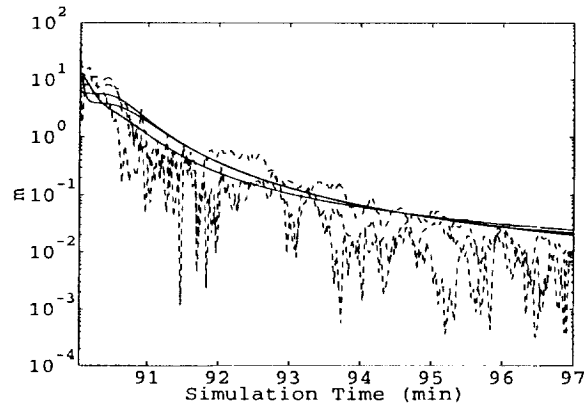


Figure 3.5.3.a: Stationkeeping Position Knowledge and Residual, 5 SVs

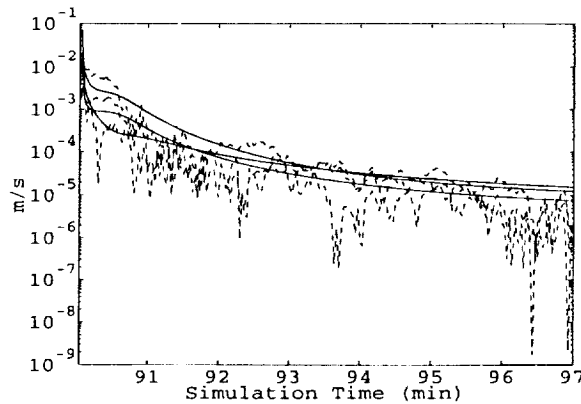


Figure 3.5.3.b: Stationkeeping Velocity Knowledge and Residual, 5 SVs

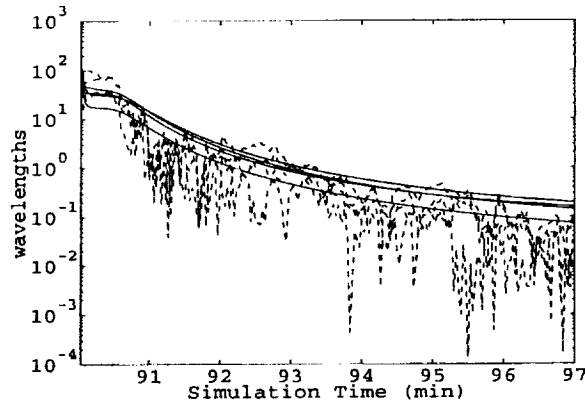


Figure 3.5.3.c: Stationkeeping Ambiguity Knowledge and Residual, 5 SVs

When only 3 GPS satellites are used in the state estimation (again with 5° measurement noise), the filter performance is clearly degraded. The convergence time is more than twice as long as when 5 or 7 SVs are used, and even then, Figures 3.5.3.d-f show that the entire state knowledge (position, velocity, and ambiguity) is an order of magnitude worse than the other cases. Thus, it is not recommended to utilize fewer than 5 GPS SVs in the differential positioning, unless 1 m uncertainty is acceptable.

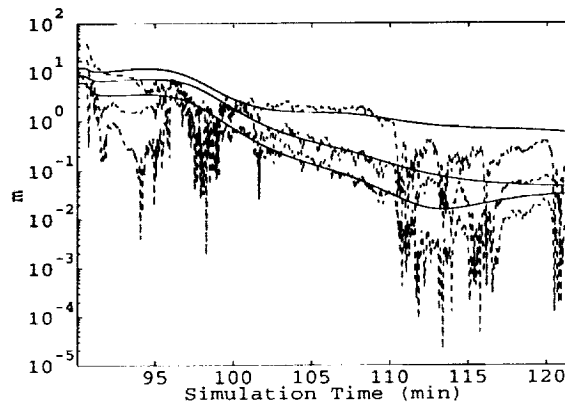


Figure 3.5.3.d: Stationkeeping Position Knowledge and Residual, 3 SVs

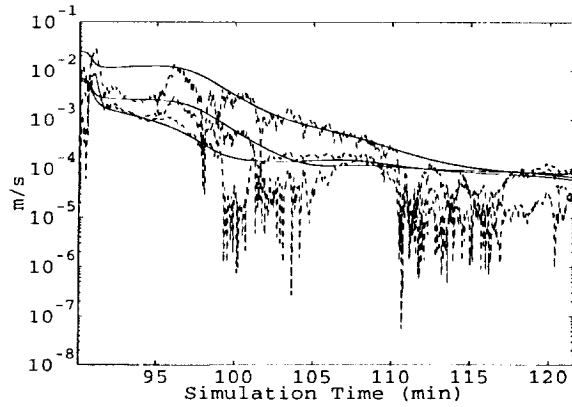


Figure 3.5.3.e: Stationkeeping Velocity Knowledge and Residual, 3 SVs

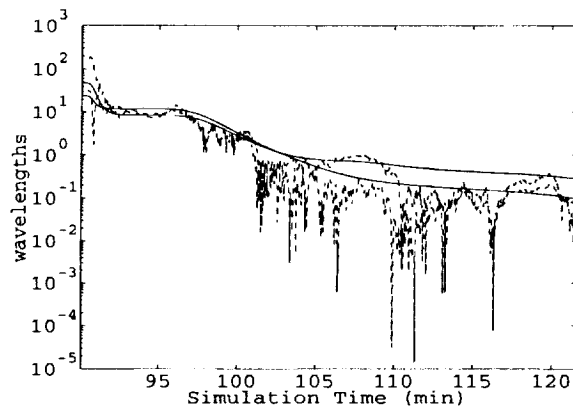


Figure 3.5.3.f: Stationkeeping Ambiguity Knowledge and Residual, 3 SVs

3.6. Stationkeeping Conclusions

This investigation of the stationkeeping phase of the rendezvous has led to several important results. First, Kinematic on the Fly GPS can be used to estimate a spacecraft's position, velocity, and integer ambiguities. Even though a twelve state system cannot be solved with seven satellites alone, the system dynamics provide additional information so that the procedure can converge. Second, the process of resolving the integer ambiguities takes about 10 minutes, less than half the time of a ground resolution. Third, using as few as 5 SVs, the filter will converge, yielding position knowledge on the order of a decimeter. Fourth, a decrease of the level of measurement noise from 15° to 5° translates into to about a three minute reduction in convergence time. Finally, obtainable final position, velocity, and ambiguity knowledge values are 0.03 m, $2 \cdot 10^{-5}$ m/s, and 0.2 wavelengths, respectively.

4. Terminal Approach via Differential GPS

4.1. Overview

The analysis of the stationkeeping phase showed that by maintaining a quasi-constant distance, the chaser and target relative positions could be determined to within a decimeter. Best results are obtained when utilizing a 7 satellite model and 5° measurement noise. For the terminal investigation, the 7 satellite method is used also. However, a conservative value of 15° measurement noise is used, partially to account for multipath errors; this is in accordance with several previous studies³². Once the integer difference ambiguities are resolved, the positions are known, and the chaser may perform a maneuver to rendezvous with the target. As with all burns, this ΔV is perturbed to account for errors in magnitude and direction. This places the chaser on a slightly incorrect trajectory, so that one or more terminal corrective burns will be required.

The Kinematic on the Fly GPS method is utilized as in the stationkeeping phase. Given that the results from the stationkeeping phase prove that the "Kinematic on the Fly" method works for the orbital system, the main question to be answered in this study is how robust this method is to cycle slips. Recall that this occurs when the receiver miscounts the carrier phase, which in turn leads to errors in the state estimate. This was not a critical topic in the stationkeeping analysis, because the target and chaser are not on an approach trajectory. Thus, if a cycle slip occurred, the ambiguity resolution procedure could be restarted without risking mission success. However, when the chaser has entered the terminal phase, it is necessary to have access to the higher accuracy of carrier phase information. If a cycle slip occurs, there may not be enough time remaining to resolve the new ambiguities. In this case, the only information available would be from C/A pseudorange measurements, but position uncertainty on the order of C/A pseudorange errors is unacceptable for rendezvous. One possible solution would be to perform a burn to stop all relative motion between the chaser and target, and to enter another stationkeeping mode to resolve the ambiguities. However, it is desired to investigate whether cycle slips can be repaired in real time; these issues, as well as typical simulation results, are discussed in the following sections.

4.2. GPS Satellite Tracking

The terminal phase is assumed to last for 45 minutes, so a constellation change will have to be made at some point in this portion of the rendezvous. The method for selecting a different set of SVs is the same as in the stationkeeping phase, described in Section 3.4, *GPS Satellite Tracking*. In addition, the same method of estimating the ambiguity and the corresponding covariance is used as in the previous phase, outlined in Section 3.3.1, *Starting Requirements*. It is important to realize that because the ambiguities were resolved in the stationkeeping phase, the chaser position is known to less than one wavelength. Therefore, when a new set of SVs is chosen, the ambiguities are basically known immediately. This will allow the chaser to continue along the trajectory to the target, with complete state knowledge, no matter how many times the selected satellites are changed.

4.3. Kinematic on the Fly GPS and Terminal Filtering

The same filtering procedure is utilized in the terminal phase as in the stationkeeping phase, described in Section 3.3, *Kinematic on the Fly GPS and Kalman Filtering*. In the stationkeeping phase, the main goal of the filtering was to resolve the integer ambiguities; this yields the relative positions needed to begin the terminal phase processing. Once the integers are known, one might argue that it is only necessary to filter the position and velocity for the terminal phase, because this represents all the needed information. However, it may be possible to utilize the Kalman filter to detect and fix cycle slips; thus, the integer states are filtered as well. Even if this method cannot be used to repair the slips, their detection alone could potentially save the mission. Knowledge that a cycle slip has occurred permits the chaser to perform a burn to enter another stationkeeping mode. In this way, the state knowledge can be reestablished, and the rendezvous continued.

The same procedures to determine the filter starting requirements are used in the terminal phase as in the stationkeeping phase. The position and velocity knowledge and states remain the same. The integer ambiguity and its covariance are determined through the procedure described in Section 3.4, *GPS Satellite Tracking*. The state and measurement noise levels are identical to those in the stationkeeping phase.

4.4. Corrective Maneuvers

The procedure for the midcourse burns in the homing phase is utilized here as well. The ΔV is assumed to be instantaneous, so that only the velocity state and covariance change. The velocity estimate after the burn is set to the nominal velocity, and the true velocity takes into account perturbations in the magnitude and direction of the burn. Upon investigating several simulations, it turns out that the terminal burn errors are extremely small, for two reasons. First, the chaser trails the target by only 2 km, so the initial burn is very small ($6 \cdot 10^{-4}$ m/s), and in turn, the initial burn errors are very small. In addition, the position is known so well at the end of the stationkeeping phase, that errors due to position uncertainty are small. Typical midcourse corrections at about 10 minutes before rendezvous are only on the order of 10^{-4} m/s. As a result, it was not deemed necessary to attempt to develop a comprehensive guidance strategy for the terminal phase; the minuscule propellant savings would not be worth it. A single maneuver about 10 minutes before rendezvous should suffice.

4.5. Terminal Phase Results

4.5.1. State Knowledge, No Cycle Slips

This section highlights the state knowledge obtainable in the terminal phase of the rendezvous. The results improve only slightly over the stationkeeping phase, most likely because of the increase in the amount of processed data. Figures 4.5.1.a-c show the state knowledge for a typical terminal phase. The position knowledge improves to around 1.3 cm, while the velocity knowledge remains around 10^{-5} m/s. The integer ambiguity knowledge increases to around $6 \cdot 10^{-2}$ wavelengths. The times of constellation change are seen most clearly in Figure 4.5.1.c, where they are shown by small discontinuities in the dotted (covariance) line at approximately 123, 130, and 139 minutes. The most

important aspect of these results is that the state knowledge can be maintained even though constellations are changed.

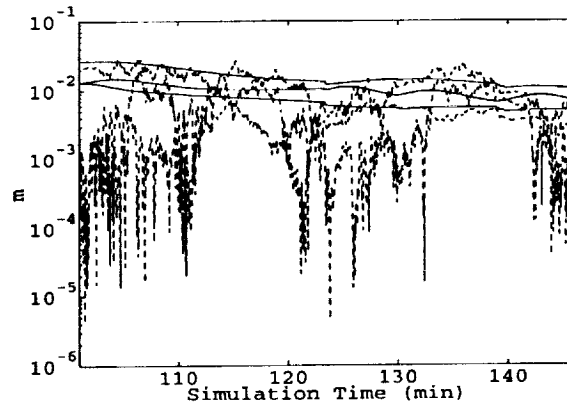


Figure 4.5.1.a: Terminal Position Knowledge and Residual

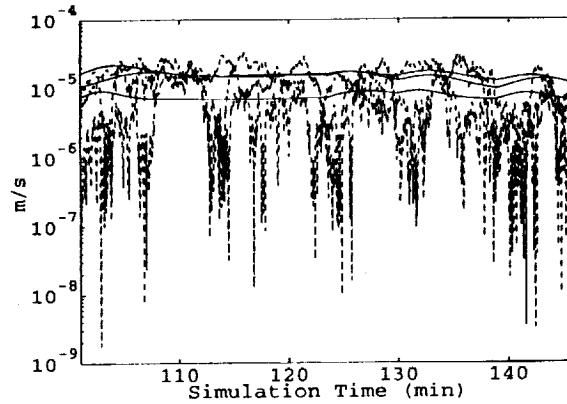


Figure 4.5.1.b: Terminal Velocity Knowledge and Residual

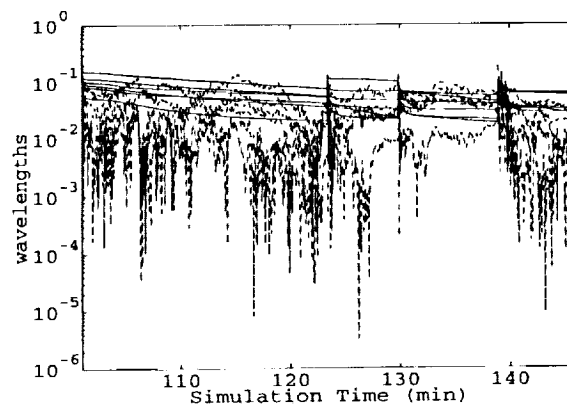


Figure 4.5.1.c: Terminal Integer Ambiguity Knowledge and Residual

4.5.2. Cycle Slips

A potentially serious event when using carrier phase relative positioning is the occurrence of a cycle slip. These are caused when the receiver zero crossing counter either misses one or more crossings, or mistakenly increments the counter. A cycle increment could be missed if there is some type of drop in signal strength; whereas an electromagnetic surge may cause the counter to increment too many cycles. The end result is that instead of position knowledge on the order of centimeters, the error is now at least one wavelength (19 cm), and possibly several wavelengths. The effect of such an occurrence on position knowledge is shown in Figure 4.5.2.a, where a cycle slip of one wavelength has been artificially inserted. Of course, it is possible that many cycles will be skipped, and as the number of skipped cycles increase, so does the position error.

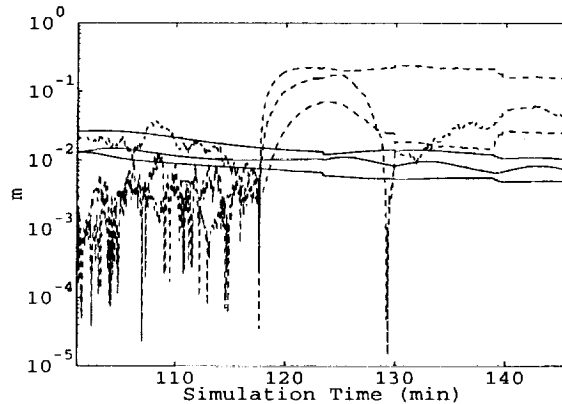


Figure 4.5.2.a: Terminal Position Knowledge and Residual, Cycle Slip at 118 Minutes

Unfortunately, the state knowledge has become so small at the time of the cycle slip that the Kalman filter basically rejects the information contained in the measurement. As a result, the filter cannot process such an occurrence on the fly, and additional logic is required. The key to detecting cycle slips lies in the examination of the measurement residual, given by

$$\Delta \mathbf{z} = \mathbf{z} - \mathbf{H}\mathbf{x} \quad (58)$$

The statistics of the measurement residual should be consistent with the measurement noise levels used in the Kalman filter. Consider, for example, the measurement residual time history for the case above, shown in Figure 4.5.2.b.

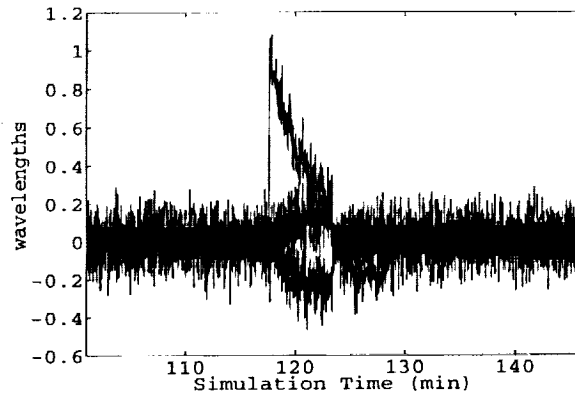


Figure 4.5.2.b: Terminal Phase Measurement Residual

The measurement residuals up to the time of the cycle slip appear to be stationary, and they are consistent with the Kalman filter measurement noise levels. Recall that the measurement noise was set at 30° , or 0.0833 wavelengths; this is the standard deviation of the measurement residuals in Figure 4.5.2.b. At the time of the cycle slip, the residual makes a significant jump, and is not at all consistent with the filter statistics. In the simulation program, the flag for a cycle slip is whenever a measurement residual lies outside the 4σ value. The choice of this value allows the simulation to ignore consistent measurement residuals outside the 3σ value, while flagging statistically inconsistent points at times of cycle slips.

An advantage of this detection method is that the measurement residual basically jumps to the number of cycles that have been skipped. Note that the residual does not jump exactly to the skipped number, because state and measurement noise is added to the system. However, simply rounding to the nearest integer should yield the correct number of skipped cycles, because the noise levels are two orders of magnitude less. Once this number is established, it is a simple matter to repair the cycle slip. Recall that the integer ambiguities are actually integer differences, so the cycle slip could have occurred on the signal from either SV. Both possibilities are checked by taking the state before the cycle slip, and propagating the Kalman filter for the one time step. The case that yields the minimum measurement residual is chosen to be truth, and the processing is continued.

The effectiveness of this procedure is highlighted in Figures 4.5.2.c-e. These show the position, integer ambiguity, and measurement residual time histories for the case above, with a cycle slip at 115 minutes. The repair scheme completely eliminates any effect of the cycle slip, thus permitting the completion of the mission.

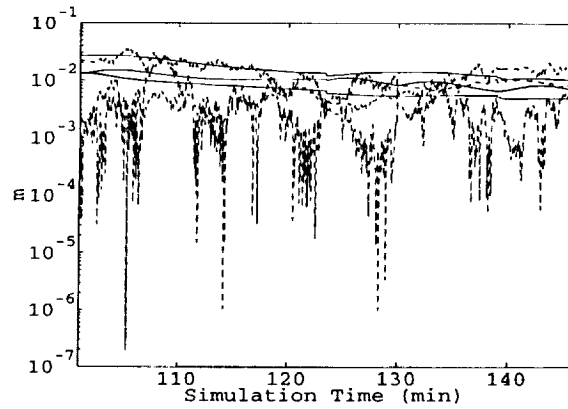


Figure 4.5.2.c: Terminal Position Knowledge and Residual, Repaired Cycle Slip

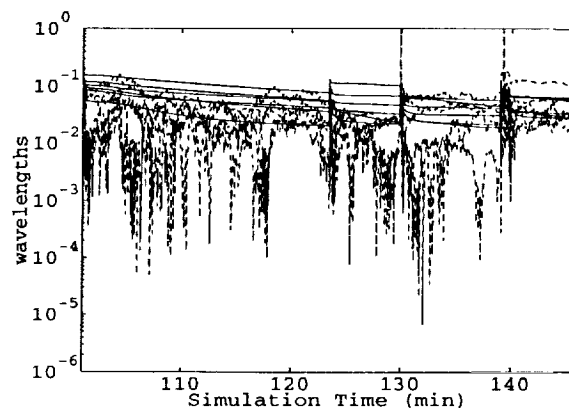


Figure 4.5.2.d: Terminal Integer Ambiguity Knowledge and Residual, Repaired Cycle Slip

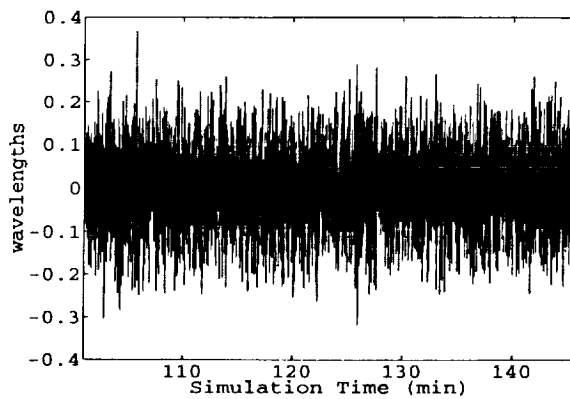


Figure 4.5.2.e: Terminal Measurement Residual, Repaired Cycle Slip

While this method was demonstrated to only one integer state and using a slip of only one cycle, it can be extended easily to apply to all states, and it is effective for any number of skipped cycles. If additional logic is incorporated, this type of method would permit a rendezvous if several or all of the integer difference states skipped any number

of cycles at any number of times. Consider for example the case where *both* phase counters contributing to the *same* integer ambiguity difference experience a cycle slip during the *same* filtering step. Because the measurements are phase differences, then at least one of the slips would show up in two separate measurements. From this second measurement, one of the cycle slips could be quantified, so that the other slip could then be determined from this new information and the first measurement. If these steps were added to the rendezvous program, then the mission would not be at risk during such an event. The possible scenarios involving the combinations of cycle slips in phase measurements become more and more complicated. However, the logic can be developed that would greatly reduce the chance of failure.

4.6. Terminal Phase Conclusions

Two major results can be reported as a result of the terminal phase investigation. First, the Kinematic on the Fly GPS method can be used for the terminal phase of the rendezvous, even though the selected SV constellation must be changed several times. Position and velocity knowledge on the order of 1 cm and 10^{-5} m/s respectively can be achieved. In addition, a method of detecting and repairing cycle slips has been demonstrated. Only a few of the many possible cycle slip scenarios have been investigated; thus, more research is required before the repair method can actually be put to use. Regardless, the detection method is valid for all cases, and is an important result in itself. If a cycle slip occurs, and it is at least detected, then a maneuver can be performed to place the chaser in a stationkeeping mode, thereby reducing mission risk.

5. GPS Attitude Determination

5.1. Overview

The investigation to this point has revealed that knowledge of the chaser position can be maintained at the centimeter level, making a rendezvous possible from this viewpoint. In addition to position knowledge, the vehicle attitude must be known accurately as well. Poor attitude knowledge can just as easily lead to mission failure as poor position knowledge. As a result, this investigation includes an analysis on utilizing GPS to determine vehicle attitude; however, an attitude control system has not been modeled. GPS attitude determination utilizes the carrier phase observable, similar to the position determination system. However, the integer ambiguity state is not needed, because of the close proximity of the receivers. The following "classic" assumptions are made in the procedure described below³³

- the spacecraft is rigid
- motions about the center of mass do not affect the motion of the center of mass
- the body frame defines the principal axes
- small rotations
- near circular orbit
- other external torques (aero, solar) are neglected

5.2. Attitude Equations of Motion

The development of the attitude mechanics for a gravity gradient stabilized satellite basically follows that presented in several references³⁴. An important difference is the reference frame convention; for this simulation, the nominal (no rotation) body frame is coincident with the instantaneous target orbital frame. Using a 3-2-1 Euler rotation (in this case, pitch - yaw - roll), the linearized equations of motion for the principal axes are

$$\begin{aligned}
 I_p \ddot{p} &= -3(I_r - I_y)n^2 p + M_p \\
 I_y \ddot{y} + (I_r + I_y - I_p)n\dot{r} + (I_p - I_r)n^2 y &= M_y \\
 I_r \ddot{r} - (I_r + I_y - I_p)n\dot{y} + (I_p - I_y)n^2 r &= -3(I_p - I_y)n^2 r + M_r
 \end{aligned} \tag{59}$$

where $I_{p,y,r}$ are the moments of inertia, n is the orbital angular velocity (mean motion), and $M_{p,y,r}$ are externally applied moments. For this investigation, the values for the moments of inertia are

$$I_p = 20 \text{ kg} \cdot \text{m}^2 \quad I_y = 6 \text{ kg} \cdot \text{m}^2 \quad I_r = 24 \text{ kg} \cdot \text{m}^2$$

Neglecting external torques, the above equations in matrix form are

$$\frac{d}{dt} \begin{Bmatrix} p \\ y \\ r \\ \dot{p} \\ \dot{y} \\ \dot{r} \end{Bmatrix} = \begin{bmatrix} 0 & 0 & 0 & 1 & 0 & 0 \\ 0 & 0 & 0 & 0 & 1 & 0 \\ 0 & 0 & 0 & 0 & 0 & 1 \\ 3n^2\alpha & 0 & 0 & 0 & 0 & 0 \\ 0 & n^2\beta & 0 & 0 & 0 & -n(1+\beta) \\ 0 & 0 & 4n^2\gamma & 0 & n(1+\gamma) & 0 \end{bmatrix} \begin{Bmatrix} p \\ y \\ r \\ \dot{p} \\ \dot{y} \\ \dot{r} \end{Bmatrix} \tag{60}$$

where

$$\alpha = \frac{I_y - I_r}{I_p} \quad \beta = \frac{I_r - I_p}{I_y} \quad \gamma = \frac{I_y - I_p}{I_r} \tag{61}$$

The solution to this set of equations is obtained through the use of the matrix exponential method. Given a set of differential equations,

$$\dot{\mathbf{x}} = \mathbf{A}\mathbf{x} \tag{62}$$

the solution $\mathbf{x}(t)$ is found from

$$\mathbf{x}(t) = e^{\mathbf{A}t} \tag{63}$$

For the Kalman filter, the attitude state transition matrix is found using this method. Knowing that the measurements are taken at intervals of Δt , the state transition matrix in between measurements is simply

$$\Phi = e^{\mathbf{A} \Delta t} \quad (64)$$

Note that because \mathbf{A} and Δt are fixed, the state transition matrix need be computed only once.

5.3. Carrier Phase Measurements

This brief discussion of carrier phase measurements is based on that found in Melvin and Hope³⁵. Given a pair of GPS antennas, the phase measured at each is given by

$$\begin{aligned} \phi_1 &= \mathbf{k}_1 \cdot \mathbf{a}_1 - \omega t \\ \phi_2 &= \mathbf{k}_2 \cdot \mathbf{a}_2 - \omega t \end{aligned} \quad (65)$$

where \mathbf{k}_i is the wave vector from the GPS satellite in question, \mathbf{a}_i is the position of the antenna phase center, ω is the circular frequency of the GPS carrier, and t is the time of the measurement. This method carries with it two important assumptions; both antennas use the same oscillator to determine the phase, and the measurements are made at the same time. In addition, if the plane wave approximation is made, and the antenna distance is assumed negligible compared to the distance to the GPS satellite, then the wave vector is given by

$$\mathbf{k}_i = \mathbf{k} = -\kappa \tilde{\rho} = -\frac{2\pi}{\lambda} \tilde{\rho} \quad (66)$$

where $\kappa=2\pi/\lambda$ is the wave number, λ is the carrier wavelength (approximately 19.0 cm for the L1 frequency), and $\tilde{\rho}$ is the unit vector from the receiver towards the GPS satellite. A phase difference is constructed from these two measurements

$$\Delta\phi = \phi_2 - \phi_1 = \mathbf{k} \cdot (\mathbf{a}_2 - \mathbf{a}_1) = \mathbf{k} \cdot \mathbf{b} \quad (67)$$

where $\mathbf{b} = (\mathbf{a}_2 - \mathbf{a}_1)$ is the baseline vector between the antennas. These phase differences are the measurements from which attitude will be determined, as described in the section below.

5.4. Attitude Determination from Carrier Phase Measurements

In order to determine vehicle attitude, this development assumes that there is a known nominal attitude that the spacecraft would traverse in the absence of perturbing forces. In the case of gravity gradient stabilization, the chaser is nominally aligned with the target orbital frame. The true attitude is then this nominal attitude plus a small deviation resulting from perturbing forces and errors. The simulation utilizes this

deviation in pitch, yaw, and roll (and their time derivatives) as the attitude state. Similarly, the measurements are deviations in the phase differences from the true and expected states. In effect, the double difference measurement is used in the attitude as well as the position determination. The only difference is that in the position determination, the double differences were between receivers and then *satellites*, whereas in the attitude determination, the differences are between the receivers and then *the true and estimated state*. The model described below is based on the developments in several references^{36, 37}.

Considering the same pair of GPS antennas above, with coordinates from the center of mass \mathbf{a}_1 and \mathbf{a}_2 expressed in the body frame, the baseline vector in the body frame, \mathbf{b}_b , is

$$\mathbf{b}_b = \mathbf{a}_2 - \mathbf{a}_1 \quad (68)$$

This baseline is assumed to be known to less than $\lambda/100$ from standard measurement techniques, including possibly static GPS measurements. This vector can be transformed to the target orbital frame via the direction cosine matrix $\boldsymbol{\varphi}$

$$\mathbf{b}_{\text{tof}} = \boldsymbol{\varphi} \mathbf{b}_b \quad (69)$$

The direction cosines are assumed to be composed of a nominal and a perturbed component, so that

$$\boldsymbol{\varphi} = \delta\boldsymbol{\varphi} \boldsymbol{\varphi}_0 \quad (70)$$

where $\boldsymbol{\varphi}_0$ is the direction cosine matrix for the nominal attitude, and $\delta\boldsymbol{\varphi}$ is the direction cosine matrix using the small angle approximation. For the 3-2-1 Euler sequence, these matrices are

$$\boldsymbol{\varphi}_0 = \begin{bmatrix} \text{CyCp} & \text{CySp} & -\text{Sy} \\ -\text{CrSp} + \text{SrSyCp} & \text{CrCp} + \text{SrSySp} & \text{SrCy} \\ \text{SrSp} + \text{CrSyCp} & -\text{SrCp} + \text{CrSySp} & \text{CrCy} \end{bmatrix} \quad (71)$$

and

$$\delta\boldsymbol{\varphi} = \begin{bmatrix} 1 & \delta p & -\delta y \\ -\delta p & 1 & \delta r \\ \delta y & -\delta r & 1 \end{bmatrix} \quad (72)$$

where S and C are sine and cosine, respectively. Upon evaluating $\boldsymbol{\varphi} = \delta\boldsymbol{\varphi} \boldsymbol{\varphi}_0$, the result can be written in the form

$$\varphi = \varphi_0 + \Delta\varphi \quad (73)$$

where

$$\begin{aligned} \Delta\varphi_{11} &= (SrSyCp - CrSp)\delta p - (SrSp + CrSyCp)\delta y \\ \Delta\varphi_{12} &= (CrCp + SrSySp)\delta p - (CrSySp - SrCp)\delta y \\ \Delta\varphi_{13} &= SrCy\delta p - CrCy\delta y \\ \Delta\varphi_{21} &= -CyCp\delta p + (SrSp + CrSyCp)\delta r \\ \Delta\varphi_{22} &= -CySp\delta p + (CrSySp - SrCp)\delta r \\ \Delta\varphi_{23} &= Sy\delta p + CrCy\delta r \\ \Delta\varphi_{31} &= CyCp\delta y - (SrSyCp - CrSp)\delta r \\ \Delta\varphi_{32} &= CySp\delta y - (CrCp + SrSySp)\delta r \\ \Delta\varphi_{33} &= -Sy\delta y - SrCy\delta r \end{aligned} \quad (74)$$

Introducing the small angle approximation into the $\Delta\varphi$ matrix yields

$$\Delta\varphi = \begin{bmatrix} 0 & \delta p & -\delta y \\ -\delta p & 0 & \delta r \\ \delta y & -\delta r & 0 \end{bmatrix} \quad (75)$$

The baseline measurement in the target orbital frame can be found from

$$\mathbf{b}_{\text{tof}} = (\varphi_0 + \Delta\varphi)\mathbf{b}_b \quad (76)$$

This result can be applied to the phase difference equation to yield

$$\Delta\phi = \mathbf{k} \cdot \mathbf{b}_{\text{tof}} = -\frac{2\pi}{\lambda} \tilde{\rho} \cdot (\varphi_0 + \Delta\varphi)\mathbf{b}_b = -\frac{2\pi}{\lambda} \tilde{\rho} \cdot \varphi_0 - \frac{2\pi}{\lambda} \tilde{\rho} \cdot \Delta\varphi\mathbf{b}_b \quad (77)$$

As stated above, a nominal attitude state is assumed; corresponding to this, there will be a nominal phase difference, $\Delta\phi_0$, and a differential phase difference, $\delta\Delta\phi$, so that the total phase difference can be expressed as

$$\Delta\phi = \Delta\phi_0 + \delta\Delta\phi \quad (78)$$

where

$$\Delta\phi_0 = -\frac{2\pi}{\lambda} \tilde{\rho} \cdot \varphi_0 \quad (79)$$

$$\delta\Delta\phi = -\frac{2\pi}{\lambda} \tilde{\rho} \cdot \Delta\phi \mathbf{b}_b$$

Because the nominal attitude is known for the entire trajectory, the nominal phase difference is known as well; hence, the quantity of interest reduces to the differential phase difference $\delta\Delta\phi$.

In order to determine how the measurement $\delta\Delta\phi$ relates to the state variables $p, y, r, \dot{p}, \dot{y}, \dot{r}$, it is necessary to determine the observation matrix. This is done by simply evaluating the above equation

$$\begin{aligned} \delta\Delta\phi &= -\frac{2\pi}{\lambda} \begin{Bmatrix} \tilde{\rho}_1 \\ \tilde{\rho}_2 \\ \tilde{\rho}_3 \end{Bmatrix} \cdot \begin{bmatrix} 0 & \delta p & -\delta y \\ -\delta p & 0 & \delta r \\ \delta y & -\delta r & 0 \end{bmatrix} \begin{bmatrix} \mathbf{b}_{b_1} \\ \mathbf{b}_{b_2} \\ \mathbf{b}_{b_3} \end{bmatrix} \\ &= -\frac{2\pi}{\lambda} \begin{bmatrix} \tilde{\rho}_1 \mathbf{b}_{b_2} - \tilde{\rho}_2 \mathbf{b}_{b_1} \\ \tilde{\rho}_3 \mathbf{b}_{b_1} - \tilde{\rho}_1 \mathbf{b}_{b_3} \\ \tilde{\rho}_2 \mathbf{b}_{b_3} - \tilde{\rho}_3 \mathbf{b}_{b_2} \end{bmatrix}^T \begin{Bmatrix} \delta p \\ \delta y \\ \delta r \end{Bmatrix} \end{aligned} \quad (80)$$

Finally, the observation matrix is

$$\delta\Delta\phi = -\frac{2\pi}{\lambda} \begin{bmatrix} \tilde{\rho}_1 \mathbf{b}_{b_2} - \tilde{\rho}_2 \mathbf{b}_{b_1} \\ \tilde{\rho}_3 \mathbf{b}_{b_1} - \tilde{\rho}_1 \mathbf{b}_{b_3} \\ \tilde{\rho}_2 \mathbf{b}_{b_3} - \tilde{\rho}_3 \mathbf{b}_{b_2} \\ 0 \\ 0 \\ 0 \end{bmatrix}^T \begin{Bmatrix} p \\ y \\ r \\ \dot{p} \\ \dot{y} \\ \dot{r} \end{Bmatrix} \quad (81)$$

or, more succinctly,

$$z = -\frac{2\pi}{\lambda} \mathbf{H} \mathbf{x} \quad (82)$$

This equation represents a single phase measurement. The incorporation of more measurements is done simply by appending rows to the observation matrix, so the final result looks something like

$$\begin{Bmatrix} \delta\Delta\phi_1 \\ \delta\Delta\phi_2 \\ \vdots \\ \delta\Delta\phi_n \end{Bmatrix} = -\frac{2\pi}{\lambda} \begin{bmatrix} \mathbf{H}_1 \\ \mathbf{H}_2 \\ \vdots \\ \mathbf{H}_n \end{bmatrix} \begin{Bmatrix} p \\ y \\ r \\ \dot{p} \\ \dot{y} \\ \dot{r} \end{Bmatrix} \quad (83)$$

This is the measurement equation that is used in the attitude Kalman filter, outlined below.

It is important to remember that a critical assumption in this formulation is that the attitude deviation from nominal is small (less than λ/b)³⁸. So long as this criterion is met, then the differential phase measurement completely defines the state of the system, and it is not necessary to take into account the integer ambiguity. However, if this assumption is violated, then the integer ambiguity must be resolved before the attitude can be positively determined. While this is certainly possible, it would increase the complexity of the model.

5.5. The Attitude Kalman Filter

The attitude Kalman filter utilizes the same procedure outlined in the previous developments. The attitude state is the deviation from nominal of the spacecraft pitch, yaw, roll, and their time derivatives

$$\mathbf{x} = [p \quad y \quad r \quad \dot{p} \quad \dot{y} \quad \dot{r}]^T \quad (84)$$

The state transition matrix is determined from the Euler 3-2-1 linearized equations of motion, as described in Section 5.2, *Attitude Equations of Motion*. Also, the observation matrix for the measurement equation is derived in Section 5.4, *Attitude Determination from Carrier Phase Measurements*. Otherwise, the filter is propagated utilizing the techniques described in Section 2.7.1, *Filtering Procedure*.

Several parameters must be specified to initialize the filter. A standard assumption is that all covariance and noise matrices are initially diagonal. The initial attitude knowledge of the chaser (the covariance matrix \mathbf{P}_0) must first be established. Assuming only coarse attitude control using gravity gradient until the rendezvous is underway, a knowledge level of 10° is assumed³⁹. The nominal state is zero attitude, so the initial truth and estimate are perturbed around this state consistent with the given initial covariance.

The main contribution to the state noise is assumed to be torques due to errors in moments of inertia. The torque due to gravity gradient effects is⁴⁰

$$T_g \approx \frac{3\mu}{R^3} I \quad (85)$$

Combining this with the relation

$$\frac{d^2\theta}{dt^2} = \frac{T}{I} \quad (86)$$

yields appropriate values for the standard deviations of the state noise and state rate noise

$$\sigma_{\theta} = \frac{3\mu}{R^3} \frac{\Delta t^2}{2} f_{\theta} \quad (87)$$

$$\sigma_{\dot{\theta}} = \frac{3\mu}{R^3} \Delta t f_{\dot{\theta}}$$

where f_{θ} and $f_{\dot{\theta}}$ are scale factors, typically set to 0.1 to account for errors in system modeling.

Because the measurement for the attitude filter is exactly the same type as for the differential filter, the same measurement noise matrix is used. As described in Section 3.3.1, *Starting Requirements*, this consists of a diagonal matrix consisting of either 15° or 5°, which is then corrected for the double differencing process by a factor of 2.

5.6. Attitude Results

5.6.1. Two Receiver Investigation

Given two GPS receivers and no other information, it is possible to determine only two of the angles describing the baseline attitude. The third angle, the rotation about the baseline vector, cannot be established. However, once the information inherent in the attitude equations of motion is applied, it is possible to estimate the third unknown angle⁴¹. For the linearized attitude equations, the roll and yaw axes are coupled; thus, measurements corresponding to one axis will be reflected in the other through the system dynamics. As a result, a baseline aligned along either the roll or yaw axis will provide information on all three angles. Consider Figures 5.6.1.a-f, which illustrate the attitude knowledge assuming a phase measurement capacity of 15°, and measurements from 4 GPS SVs. For each case, the knowledge of the observable axes starts around 1° for the homing phase, and decreases to about 0.1° for the terminal phase. For the unobservable axis, the knowledge seems to depend on which baseline was used. For the roll aligned antenna, the knowledge starts around 200° and falls to about 10°; the yaw aligned antenna begins at the same level, but falls to around 1°. For both cases, this poor knowledge eliminates the use of only two receivers for an attitude control system.

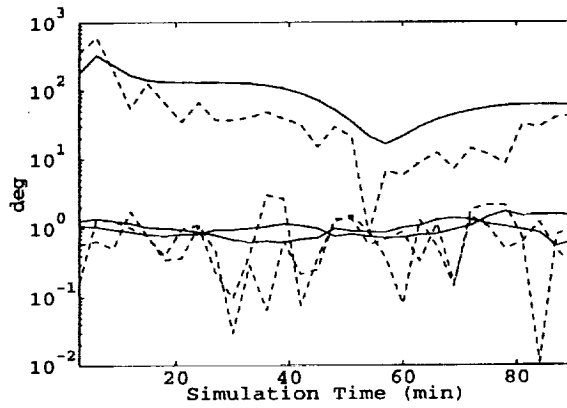


Figure 5.6.1.a: Homing Attitude Knowledge and Residual, Roll Aligned Antenna

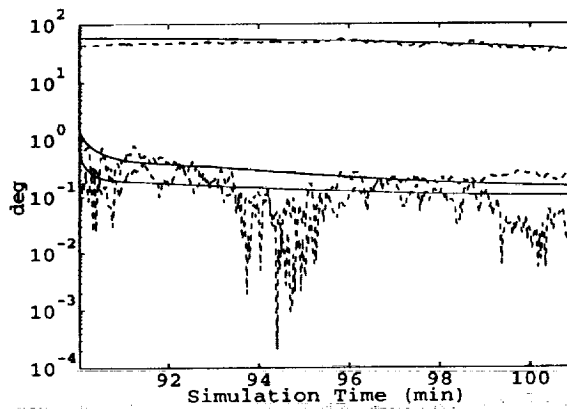


Figure 5.6.1.b: Stationkeeping Attitude Knowledge and Residual, Roll Aligned Antenna

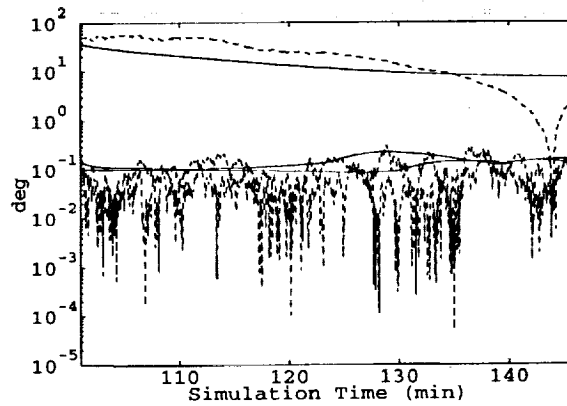


Figure 5.6.1.c: Terminal Attitude Knowledge and Residual, Roll Aligned Antenna

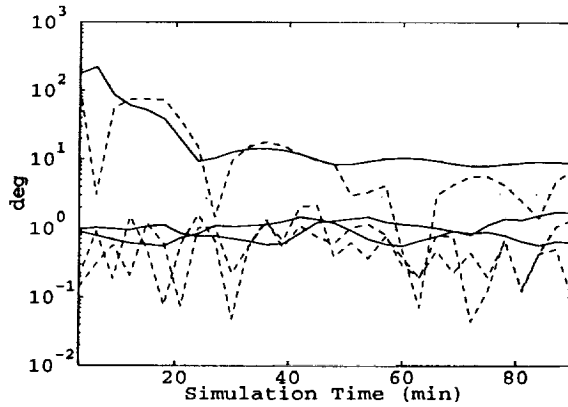


Figure 5.6.1.d: Homing Attitude Knowledge and Residual, Yaw Aligned Antenna

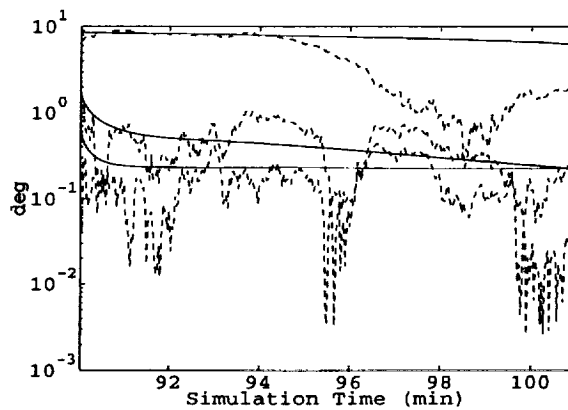


Figure 5.6.1.e: Stationkeeping Attitude Knowledge and Residual, Yaw Aligned Antenna

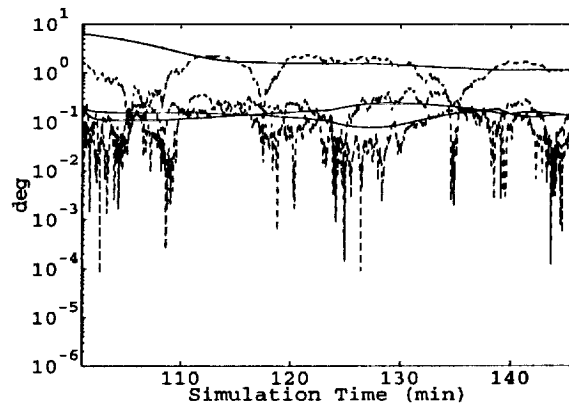


Figure 5.6.1.f: Terminal Attitude Knowledge and Residual, Yaw Aligned Antenna

Unlike the other two axes, the pitch angle is not coupled with any other motion. Hence, if the baseline vector is oriented along the pitch axis, it is impossible to observe motion about that axis. This is clear in Figures 5.6.1.g-i; the pitch axis is completely inestimable. However, the knowledge of the remaining axes falls from about 1° in the homing phase to about 0.1° in the terminal phase. An interesting point to note is the

oscillatory nature of the pitch residual; this phenomenon is consistent with the pitch period.

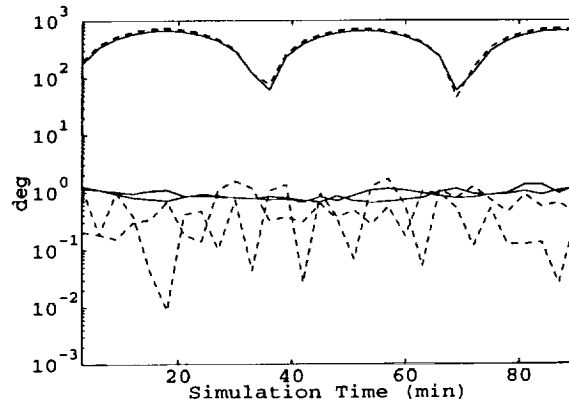


Figure 5.6.1.g: Homing Attitude Knowledge and Residual, Pitch Aligned Antenna

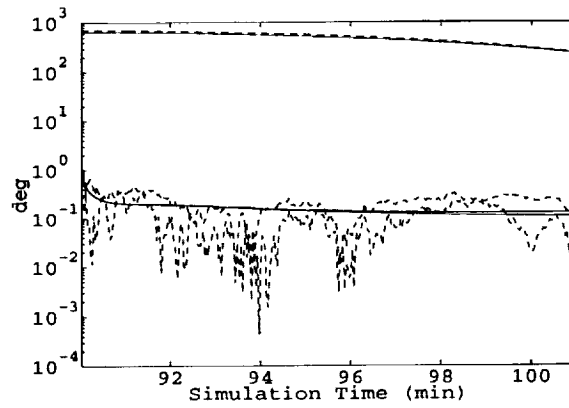


Figure 5.6.1.h: Stationkeeping Attitude Knowledge and Residual, Pitch Aligned Antenna

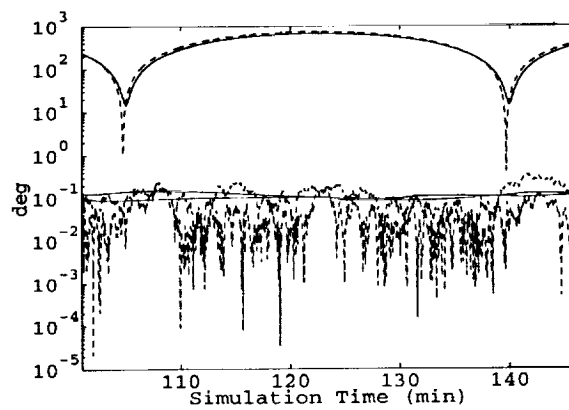


Figure 5.6.1.i: Terminal Attitude Knowledge and Residual, Pitch Aligned Antenna

5.6.1.1. The Use of More GPS Satellites

All of the above results utilize measurements from four GPS satellites. It is conceivable that more measurements could improve the attitude knowledge, so the effect of utilizing 6 SVs was investigated. Figure 5.6.1.1.a shows that while there is a small gain in the observable directions, the unobservable axis is still too poor to utilize for a control system. While this figure only shows the stationkeeping phase of the rendezvous, the results are similar for the homing and terminal phases.

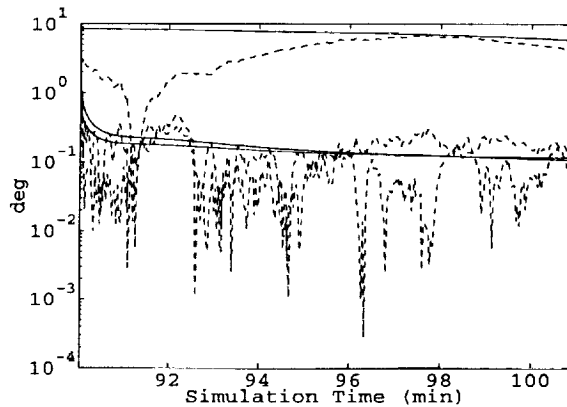


Figure 5.6.1.1.a: Stationkeeping Attitude Knowledge and Residual, 6 GPS SVs

5.6.1.2. Increasing the Phase Measurement Accuracy

If the measurement noise levels are reduced from 15° to 5° , while using 4 SVs, the state estimates should of course increase in accuracy; the question remains whether the use of only a pair of GPS antennas will supply enough accuracy in all dimensions for use in a control system. Figure 5.6.1.2.a-c show the results of this investigation. During the homing phase, the attitude knowledge in the unobservable direction still remains on the order of 10° ; however, the knowledge of the remaining axes is established at about 0.5° . In the stationkeeping and terminal phases, the accuracy of the observable axes falls to slightly below 0.1° . The largest increase is evident in the unobservable axis; its knowledge falls to the order of 1° .

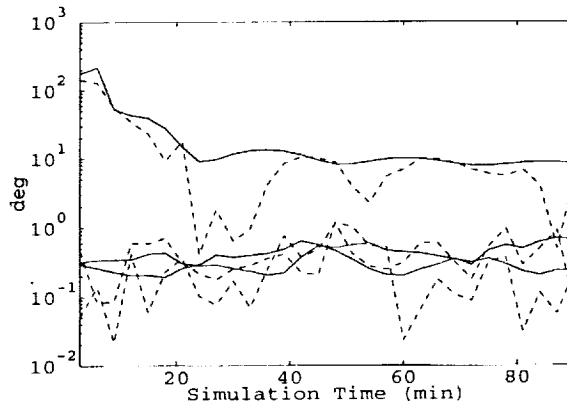


Figure 5.6.1.2.a: Homing Attitude Knowledge and Residual, 5° Measurement Noise

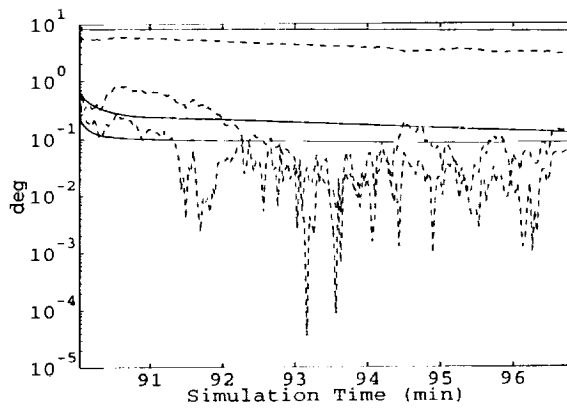


Figure 5.6.1.2.b: Stationkeeping Attitude Knowledge and Residual, 5° Measurement Noise

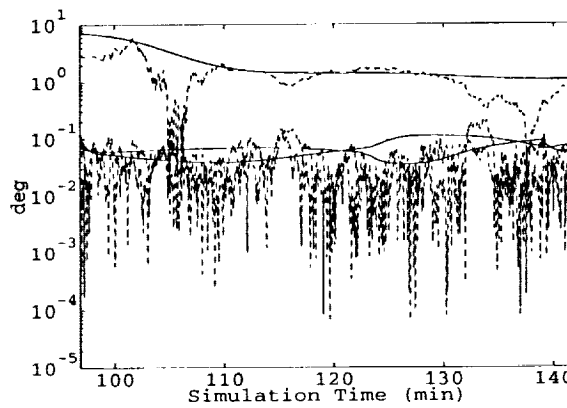


Figure 5.6.1.2.c: Terminal Attitude Knowledge and Residual, 5° Measurement Noise

5.6.2. Three Receiver Investigation

In this section, the use of three GPS antennas is considered. In this way, more than one baseline vector is available, thus eliminating the problem of the unobservable

angle seen in the above sections. Three GPS SVs are utilized, providing three double differences across two different baselines for a total of six measurements.

5.6.2.1. Phase Measurement Capacity: 15°

For even the worst case measurement noise values, the results are very promising, as shown in Figures 5.6.2.1.a-c. The knowledge of all three attitude angles is maintained on the order of 1° for the entire homing phase. The estimates improve in the stationkeeping and terminal phases, to around 0.1° , three axis.

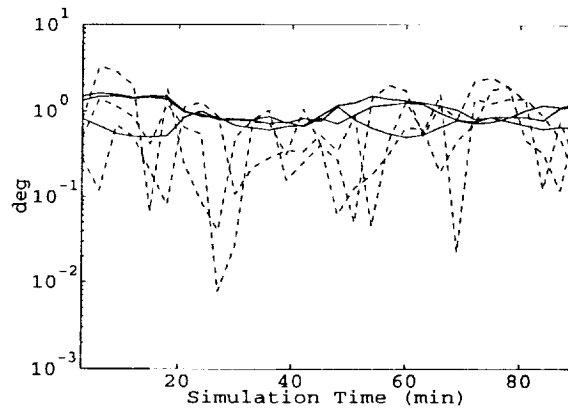


Figure 5.6.2.1.a: Homing Attitude Knowledge and Residual, Three Antenna

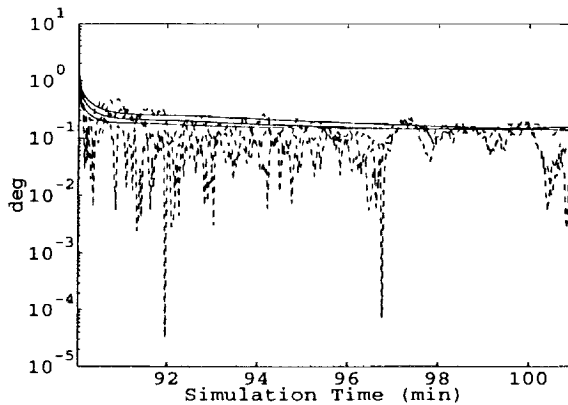


Figure 5.6.2.1.b: Stationkeeping Attitude Knowledge and Residual, Three Antenna

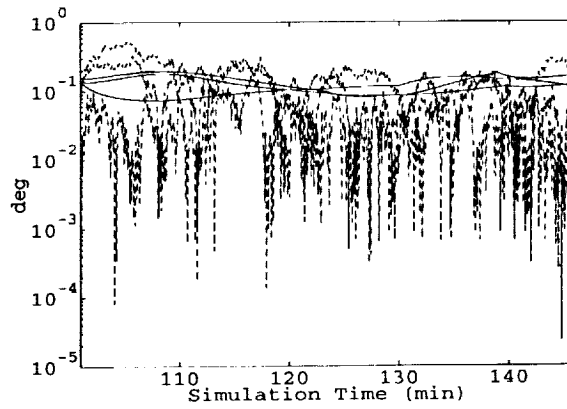


Figure 5.6.2.1.c: Terminal Attitude Knowledge and Residual, Three Antenna

5.6.2.2. Phase Measurement Capacity: 5°

The decreased measurement noise directly affects the knowledge of the attitude state. As with the 15° case, all three states are estimated consistently due to the inclusion of the third antenna; this is shown in Figures 5.6.2.2.a-c. However, the lower levels of noise lead to homing phase attitude knowledge on the order of 0.3° , falling to about 0.05° in the terminal phase.

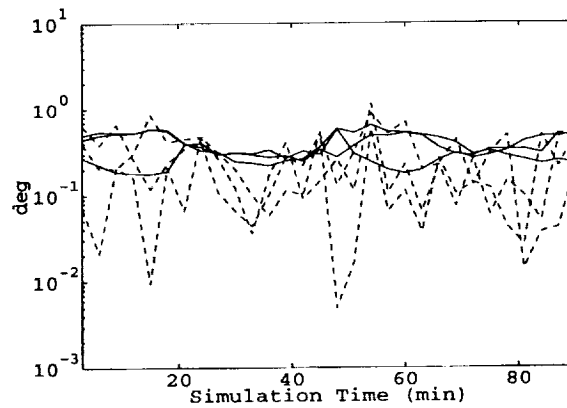


Figure 5.6.2.2.a: Homing Attitude Knowledge and Residual, Three Antenna

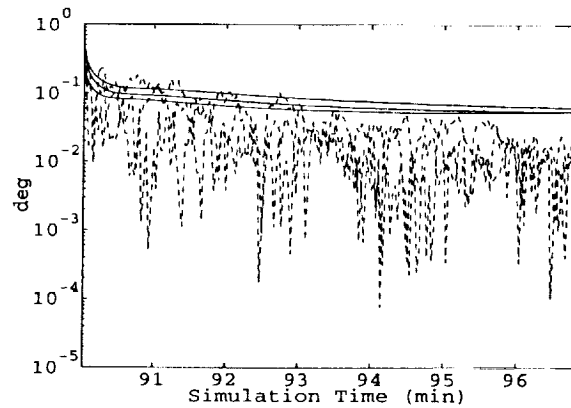


Figure 5.6.2.2.b: Stationkeeping Attitude Knowledge and Residual, Three Antenna

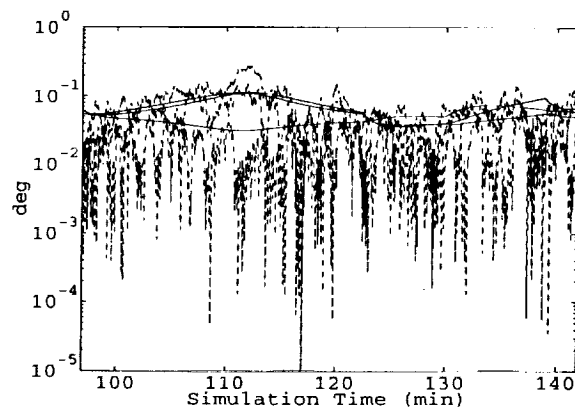


Figure 5.6.2.2.c: Terminal Attitude Knowledge and Residual, Three Antenna

5.7. Attitude Determination Conclusions

The main consequence of this investigation is that GPS can be utilized to determine the attitude of a spacecraft to within about 0.05° . Several other results can be reported as well. For example, it is possible to use only two GPS receivers, coupled with the attitude dynamics, to determine spacecraft attitude. The best case scenario was when the baseline was along the yaw axis, yielding knowledge on the order of 1° . However, this two receiver method is not recommended for use in an attitude control system, even if more SVs are used or the measurement noise level is decreased. Also, if three GPS receivers are utilized, then full attitude knowledge can be obtained. If a 15° measurement noise level is used, the attitude knowledge converges to about 0.1° ; whereas, if a 5° measurement noise level is used, 0.05° is the result.

6. Summary and Recommendations

This study has investigated a wide variety of areas in the use of GPS for automated rendezvous and docking. The main result is that it is possible to utilize GPS alone for the position and attitude determination of such a mission. It is important to realize that a simulation of the actual docking procedure has not been created; thus it is

not appropriate to directly compare rendezvous control requirements and the knowledge achievable from GPS. However, the GPS state knowledge must be better than the control requirements, or else the GPS system cannot be used. Thus, assuming that the requirements for a rendezvous are those shown in Table 6.a, state knowledge from GPS has been shown to exceed the necessary values, consistent with the assumptions in this investigation.

Table 6.a: Rendezvous Control Requirements and GPS Knowledge

	Control Requirements ¹⁴²	<u>GPS Knowledge</u>
Lateral Misalignment	7.5 cm	1 cm
Docking Speed	20 mm/s	0.01 mm/s
Angular Offsets	1.5°	0.05°

Of course, it is advisable to include redundant systems, perhaps other than GPS based, to ensure mission safety. This section will briefly highlight some other results, and outline subjects that require further research.

This work has shown that the use of the Kalman filter is appropriate for the homing phase of a rendezvous, even in the presence of selective availability. State knowledge on the order of 20-30 m is obtainable using C/A code positioning. The Kalman filter was also demonstrated to be applicable to the resolution of the integer ambiguities in the stationkeeping mode, and to the accurate estimation of the state in the terminal phase. Position and velocity knowledge on the order of 1 cm and 10^{-5} m/s respectively can be achieved at rendezvous. In the homing phase, guidance strategies and the effects of mismodeling SA statistics were investigated. "Kinematic on the Fly" GPS was analyzed in the stationkeeping phase; it was proven to be applicable, even when using as few as 5 SVs. Cycle slips were examined in the terminal phase, and a method of at least detecting such a slip, if not repairing it, was demonstrated. Attitude knowledge on the order of 0.05° was shown to be achievable.

While this research has laid a strong foundation for the use of GPS in a rendezvous mission, there still remain many areas that need to be investigated further. For example, this study assumed that the SA noise was stationary with zero mean; however, this may not always be true. Also, the use of a sequential filter may not be entirely appropriate when attempting to estimate integers; as mentioned previously, the use of a batch filter may be more advantageous. In the discussion of cycle slips, a method of detecting such an occurrence was shown. This knowledge allowed the cycle slip to be repaired, and the state knowledge to be maintained. However, a more in depth investigation into the logic to repair concurrent cycle slips (on one or more channels) must be performed. In addition, this research utilized larger phase measurement errors to compensate for possible multipath errors; if a more exact multipath model could be developed and utilized, system errors could be reduced. Further, the use of an "all in view" method of positioning could result in decreased error levels. Finally, the effects of uncertainties in the positions of the GPS SVs, perhaps due to a ground station failure, could be investigated. All of these areas and more require further research before the methods explored in this study can be implemented in an actual rendezvous mission.

Appendix A: Description of Computer Programs

A.1. Overview

The computer programs used in this study were developed on an IBM 486/50DX machine. The code was written in the MATLAB 4.0 for Windows programming environment. Three main driver programs have been developed which address the needs of this investigation:

- 1) SA - generates the selective availability data via the Braasch model
- 2) RVLOOKUP - creates the lookup tables with the GPS SV state information
- 3) GOMONTE - simulates the rendezvous, using GPS position and attitude determination, from homing through terminal phases

These drivers call the necessary subroutines to perform whichever task is desired. An outline of the control flow for each program is included below; each successive indentation represents a deeper level of subroutines. All programs and subroutines are discussed in greater detail in the following section.

Program 1

SA

Program 2

RVLOOKUP

 KEPLER

 FGC

 FCTORIAL

 FGS

 FCTORIAL

 MDLOS

 ANGBET

 CROSS

 D2R

 R2D

 ORB2XYZ

 D2R

 DCM313

 R2D

Program 3

GOMONTE

 ATTSTMC

 CROSS

 D2R

 DETVEL

GMPARMS
RVMONTE
 ATTOBSM
 GPSMEAS
 GPSEQNS
 PHAS1SAV
 PHAS2SAV
 PHASEND
 RNDVECMT
 RV_SK
 ATTOBSM
 ATTSTMC
 GPSMEAS
 GPSEQNS
 PHASESVS
 R2D
 RNDVECMT
 RVKALM
 RNDVECMT
 RVLOC2E
 CROSS
 STATNOIS
 STMATRIX
 TRMOBSM
RVCSTAT
 STMATRIX
RVDELTA
 CROSS
 DETVEL
RVDOPSUB
 GDOP4
 AREATRI
 VOLTETRA
RVINIT
 RNDVECMT
 RVDELTA
 CROSS
 DETVEL
RVKALM
 RNDVECMT
RVLOC2E
 CROSS
RVSVLOS
 MDLOS
 ANGBET

CROSS
 D2R
 R2D
 RVTERM
 ATTOBSM
 GPSMEAS
 GPSEQNS
 PHASESVS
 R2D
 RNDVECMT
 RVDELTA
 CROSS
 DETVEL
 RVKALM
 RNDVECMT
 RVLOC2E
 CROSS
 STATNOIS
 STMATRIX
 TRMOBSM
 STATNOIS
 STMATRIX

A.2. Alphabetical Subroutine List and Description

This section lists alphabetically all the subroutines used in the rendezvous simulation; a brief summary of each is included as well. All input and output variables are listed and described. Where necessary, the dimensions of matrices are explained in parenthesis following the variable description; for example, the parenthesis $(x, y, z \times SV_1, SV_2, SV_3, \dots)$ indicate that the three rows of the matrix are $x, y,$ and z positions, while the columns refer to the satellites $SV_1, SV_2,$ and so forth. Unless otherwise mentioned, all routines use as standard units kilograms, kilometers, and seconds.

ANGBET - This function calculates the angle between two vectors, in radians.

Inputs:

x, y - two 3×1 vectors

Outputs:

z - the angle between x and y , in radians

AREATRI - This function calculates the area of the triangle formed from three endpoints.

Inputs:

a, b, c - the 3D endpoints of the triangle

Outputs:

x - the area of the triangle

ATTOBSM - This function calculates the attitude observation matrix, for use in the attitude Kalman filter.

Inputs:

ant_dist - distance between the receiver antennas, km
ant_vect - unit vector from one antenna to the other
wavelen - phase wavelength to use, km (standard L1 = 19.0 cm)
bvec2sat - matrix of unit vectors to the 4 GPS SVs (x, y, z × SV₁, SV₂, SV₃, SV₄)

Outputs:

att_hcalc - the attitude observation matrix

ATTSTMC - This function calculates the attitude state transition matrix.

Inputs:

mom_in - moments of inertia, kg/km²
dt - time between measurements, sec
mu - earth gravitational parameter, km³/s²
sc_rad - radius of the target (rendezvous radius), km

Outputs:

stm - attitude state transition matrix

CROSS - This function returns the cross product of two 3D vectors.

Inputs:

x, y - two 3×1 column vectors

Outputs:

z - x×y

D2R - This function converts degrees to radians.

Inputs:

x - angle in degrees

Outputs:

y - angle in radians

DCM313 - This function returns the direction cosine matrix for a 3-1-3 rotation.

Inputs:

ang1, ang2, ang3 - Euler angles in radians

Outputs:

y - DCM

DETVEL - This function determines the velocity necessary to arrive at the origin in the desired time.

Inputs:

pos - position vector, km
w - orbital angular velocity of target, rad/s
tott - total travel time, sec

Outputs:

vel - the velocity vector necessary to perform the maneuver, km/s

FACTORIAL - This function calculates the factorial of an integer.

Inputs:

x - integer

Outputs:

y - x!

FGC - This function is used in the universal variables approach to orbit propagation; it is only called by the KEPLER function.

Inputs:

z

Outputs:

C(z)

FGS - This function is used in the universal variables approach to orbit propagation; it is only called by the KEPLER function.

Inputs:

z

Outputs:

S(z)

GDOP4 - Given the unit vectors from the chaser to the four selected SVs, this function calculates the associated GDOP.

Inputs:

a, b, c, d - the unit vectors from the chaser to the four selected SVs

Outputs:

x - the associated GDOP

GMPARMS - This routine specifies the desired simulation parameters. These parameters include everything, from the elevation angle to the phase measurement noise level to the number of Monte Carlo runs.

GOMONTE - This is the main rendezvous simulation driver program. It calls all the necessary functions to determine both position and attitude in all phases of the rendezvous; this includes line of sight calculations, triangulations, etc. It can perform either a single simulation or a multi-run Monte Carlo simulation. The user inputs are defined in the routine GMPARMS.

GPSEONS - This function solves the GPS system of equations: 4 equations in 4 unknowns, i.e. position (x, y, z) and clock offset.

Inputs:

xyztges - initial guess of position and clock offset, km and sec

svpos - positions of the four SVs, km (x, y, z × SV₁, SV₂, SV₃, SV₄)

svrng - pseudoranges to the four SVs

rngtol - tolerance to iterate RANGE part to (i.e., 1 part in 1e-6)

Outputs:

xyzt - solution to the 4 nonlinear GPS equations, km and sec

meascov - the $\text{inv}(A) \cdot \text{inv}(A)'$ matrix necessary to transform the covariance properly in the Kalman filter

GPSMEAS - This function returns the actual position measurement (x, y, z) calculated from GPS; this includes the effects of SA.

Inputs:

svsoln - the positions of the 4 GPS satellites to be used in triangulation, km (x, y, z \times SV₁, SV₂, SV₃, SV₄)

rtgt - the position of the origin of the local frame (i.e., the target position), km

vtgt - the velocity of the origin of the local frame (i.e., the target position), km

x - the position of the chaser in local coordinates, km

sa - the SA noise values for the 4 satellites

rngtol - the position tolerance to iterate to

ijk2loc - DCM from inertial to local coordinates

loc2ijk - DCM from local to inertial coordinates

Outputs:

gpsz - the actual GPS measurement (with SA), km

meascov - the $\text{inv}(A) \cdot \text{inv}(A)'$ matrix necessary to transform the covariance matrix properly for the Kalman filter

bvec2sat - the unit vectors from the receiver to the satellites, for use in the attitude observation matrix

KEPLER - This subroutine is a standard orbit propagator; it uses the universal variables approach developed in Bate, Mueller, and White.

Inputs:

r0 - initial position vector, km (3 \times 1)

v0 - initial velocity vector, km/s (3 \times 1)

dt - time to propagate orbit, sec

mu - gravitational parameter, km³/sec²

proptol - tolerance to iterate to find final r,v

propiter - maximum number of iterations

Outputs:

r - position vector after time dt, km

v - velocity vector after time dt, km/sec

MDLOS - Given the receiver position and the SV position, this subroutine determines whether or not a line of sight exists.

Inputs:

sc_vec - the position of the observer, km

sv_vec - the position of the satellite you're trying to see, km

elevmask - the elevation angle from the earth tangent, deg

alt - the altitude of the observer, km

Outputs:

los - 0 - not in view, 1 - in view

ORB2XYZ - Given the orbital elements of a body, as well as the gravitational parameter, this routine calculates the corresponding position and velocity vectors. This subroutine accepts several different possible combinations of orbital elements; however, a flag must be set to indicate which set is being used.

Inputs:

inputmode - which orbital element set is being used

mu - gravitational parameter, km^3/sec^2

r - radius vector, km

v - velocity vector, km/sec

Outputs:

orbelem - orbital elements output matrix

flag - orbit descriptor

PHAS1SAV - This program saves and then removes values at the end of the homing phase that are not needed in subsequent phases, thereby saving computer memory space.

PHAS2SAV - This program saves and then removes values at the end of the stationkeeping phase that are not needed in subsequent phases, thereby saving computer memory space.

PHASEND - This program saves and then removes values at the end of the terminal phase that are not needed in subsequent phases, thereby saving computer memory space.

PHASESVS - This routine calculates which seven SVs stay in sight the longest from the current time; it is used in the carrier phase positioning in the stationkeeping and terminal phases.

Inputs:

svlos - the line of sight matrix; 0-not in sight, 1-in sight (time \times SV₁, SV₂, SV₃, SV₄, ...)

Outputs:

long_svs - the SVs that stay in view the longest

sv_times - the times from current that the SVs will drop out of sight, sec

R2D - This function converts radians to degrees.

Inputs:

x - angle in radians

Outputs:

y - angle in degrees

RNDVECMT - This function returns an error vector consistent with the statistics of the covariance matrix p.

Inputs:

p - covariance matrix

Outputs:

randvect - error vector consistent with p

RV-SK - This is the main simulation routine for the stationkeeping section of the rendezvous. Based on the results from the homing phase, this routine calls the necessary programs to calculate the integer ambiguities, propagate the Kalman filter, and so forth. At the completion of this phase, the driver for the terminal section is called (RVTERM).

RVCSTAT - This function calculates a variety of statistics on the C/A positioning.

Inputs:

tott - total time in the homing phase, sec

tremain - time remaining in the homing phase, sec

w - angular frequency of the target orbit, rad/sec

p - current covariance matrix

phi - DCM from inertial to b-plane

x - current state truth

xhat - current state estimate

Outputs:

stats - the diagonals of the covariance projected to the b-plane time of arrival

covdiag - diagonal elements of covariance matrix

xprojstate - the true state projected to b-plane arrival

projstate - the estimated state projected to b-plane arrival

sumcov - the harmonic mean (cube root of the product of the diagonal) of the position 3x3 covariance, projected to the b-plane time of arrival

sumcov3 - not used

xrerr - the truth radial error at b plane arrival, km

rerr - the estimated error at b plane arrival, km

dist - the current estimated distance to the target, km

RVDELTA V - This function simulates a ΔV maneuver. Based on the desired velocity increment, the *new* true and estimated velocities are calculated, as well as the new velocity covariance.

Inputs:

tott - the total time in the homing phase, sec

tremain - the time remaining in the homing phase, sec

xold - true state before the maneuver

xhatold - estimated state before the maneuver

pold - covariance matrix before the maneuver

w - the orbital angular velocity, rad/sec

burnmagpct - the percent error in the magnitude of the burn

burnxpct - the percent error in the cross directions of the burn
mode - 1 - the maneuver is to put the chaser on a rendezvous trajectory with the target
2 - the maneuver is to stop relative motion between chaser and target (i.e., at the beginning of the stationkeeping phase)

Outputs:

x - true state after the maneuver
xhat - estimated state after the maneuver
p - covariance matrix after the maneuver
normdv - the magnitude of the ΔV

RVDOPSUB - Given the SVs in sight, this function determines the sub optimal combination of four (via the Noe, Myers, and Wu method) to use in the position determination.

Inputs:

svlos - the row vector of true or false (1 or 0) line of sight
svpos - the row vector of all SV positions, km ($SV_{1x}, SV_{1y}, SV_{1z}, SV_{2x}, SV_{2y}, \dots$)
rtgt - the coordinates of the origin, km
x - estimate of chaser position in inertial coordinates, km
ijk2loc - DCM between inertial and local coordinates

Outputs:

svs - the four SVs to use in position determination
svsoln - the row vector of the positions of the selected four SVs, km ($SV_{1x}, SV_{1y}, SV_{1z}, SV_{2x}, SV_{2y}, \dots$)
gdop - the GDOP value for the selected four SVs

RVINIT - This subroutine basically performs a variety of initialization procedures. All the necessary variables for the computer simulation are created, and some of the default values are calculated.

RVKALM - This function is a generic Kalman filter propagator. It accepts a *mode* variable that allows for special treatment of individual cases, such as SA incorporation or cycle slip repair.

Inputs:

mode - 2=no SA, 3=SA, 4=Gaussian SA, 22=cycle slip repair, 999=attitude
stm - state transition matrix
x - truth state
xhatold - last state estimate
pold - last covariance matrix
q - state noise covariance matrix
r - measurement noise covariance matrix
h - observation matrix
gpsz - actual GPS measurements

Outputs:

xhat - new state estimate
z - measurements
p - new covariance matrix

RVLOC2E - This function determines the direction cosine matrices from local to inertial frames and vice versa.

Inputs:

rtgt - the position of the origin of the local frame (i.e., the target position), km
vtgt - the velocity of the origin of the local frame (i.e., the target position), km

Outputs:

ijk2loc - DCM from inertial to local
loc2ijk - DCM from local to inertial

RVLOOKUP - This program creates the lookup tables for the GPS satellite positions and velocities, as well as the target orbit, if desired. These lookup tables are stored and then used by GOMONTE to avoid doing those calculations repeatedly.

Inputs:

orbelem - orbital elements of the target ($p, e, i, \Omega, \omega, \nu$)
dt - time increment, sec
endtime - total time to generate tables for, sec
svelem - the elements of the GPS SVs ($SV_1, SV_2, SV_3, \times p, e, i, \Omega, \omega, \nu$)
elevang - the desired elevation angle, deg
calctgt - flag to calculate the target states or not

Outputs:

rtgt - positions of the target, km (time \times x, y, z)
vtgt - velocities of the target, km/s (time \times x, y, z)
svpos - positions of the SVs, km (time \times $SV_{1x}, SV_{1y}, SV_{1z}, SV_{2x}, SV_{2y}, SV_{2z}, \dots$)
svvel - velocities of the SVs, km/s (time \times $SV_{1x}, SV_{1y}, SV_{1z}, SV_{2x}, SV_{2y}, \dots$)
svlos - line of sight from target to SV, 1 = los, 0 = no los (time \times $SV_{1x}, SV_{1y}, SV_{1z}, SV_{2x}, SV_{2y}, SV_{2z}, \dots$)

RVMONTE - This program performs one rendezvous simulation, from the homing through the terminal phases. Utilizing GPS for position and attitude determination, Kalman filters are used to determine all desired outputs. It is called by GOMONTE, which is basically a loop to perform the rendezvous for Monte Carlo simulations.

RVSVLOS - This function determines which SVs in the constellation are in view.

Inputs:

x - current true state
svpos - the row vector containing the positions of the GPS SVs, km ($SV_{1x}, SV_{1y}, SV_{1z}, SV_{2x}, SV_{2y}, SV_{2z}, \dots$)
elevang - the desired elevation angle from the earth tangent, deg
alt - the altitude of the rendezvous, km

OUTPUTS:

svlos - the line of sight for all SVs, 1 = in sight, 0 = out of sight

SA - This program calculates the selective availability residuals via the Braasch method.

Inputs:

blocklen - the length of time to create SA, sec
numblock - the number of time histories to create
userdt - the increment to output the SA in seconds, i.e., 60 = 1 min
increments, 120 = 2 min increments

Outputs:

sares - matrix of SA residuals (time×blocks)
sares2 - matrix of SA residuals (time×blocks)
tsares - time index based on userdt

STATNOIS - This function calculates the state noise for the Kalman filter, based on a specified percent unknown in the acceleration due to drag at the rendezvous altitude.

Inputs:

w - orbital angular velocity, rad/sec
r - rendezvous altitude, km
dt - measurement intervals, sec
dragpct - the percent of acceleration due to drag to use

Outputs:

possn - position state noise, km
velsn - velocity state noise, km/sec

STMATRIX - This function calculates the chaser state transition matrix based on the linearized relative equations of motion.

Inputs:

t - measurement intervals, sec
w - orbital angular velocity, rad/sec

Outputs:

stm - state transition matrix over the time interval t

TRMOBSM - This function calculates the observation matrix for use in the Kalman filtering during the stationkeeping and terminal portions of the rendezvous.

Inputs:

h - the matrix of unit vectors to the SVs ($SV_1, SV_2, SV_3, \dots \times x, y, z$)

Outputs:

H - the observation matrix

VOLTETRA - This function calculates the volume of the tetrahedron formed from four points.

Inputs:

a, b, c, d - the four points forming the tetrahedron

Outputs:

x - the associated volume

References

- ¹G.B. Green, P.D. Massatt, N.W. Rhodus, "The GPS 21 Primary Satellite Constellation", *Navigation: Journal of The Institute of Navigation*, Vol. 36, No. 1, Spring 1989, pp. 10-11.
- ²B. Hofmann-Wellenhof, H. Lichtenegger, J. Collins, *GPS: Theory and Practice*, 1st ed., Springer-Verlag, 1993, pp. 13-25.
- ³R.G. Brown, Patrick Y.C. Hwang, *Introduction to Random Signals and Applied Kalman Filtering*, 2nd ed., John Wiley & Sons, 1992, pp. 409-411.
- ⁴V.A. Chobotov (ed.), *Orbital Mechanics*, American Institute of Aeronautics and Astronautics, 1991, p. 178.
- ⁵V.A. Chobotov (ed.), *Orbital Mechanics*, American Institute of Aeronautics and Astronautics, 1991, p. 179.
- ⁶V.A. Chobotov (ed.), *Orbital Mechanics*, American Institute of Aeronautics and Astronautics, 1991, p. 179.
- ⁷R.R. Bate, D.D. Mueller, J.E. White, *Fundamentals of Astrodynamics*, Dover Publications, Inc., 1971, pp. 191-222.
- ⁸G.B. Green, P.D. Massatt, N.W. Rhodus, "The GPS 21 Primary Satellite Constellation", *Navigation: Journal of The Institute of Navigation*, Vol. 36, No. 1, Spring 1989, p. 15.
- ⁹K. Rektorys (ed.), *Survey of Applicable Mathematics*, The M.I.T. Press, 1969, p. 245.
- ¹⁰P. Massatt, K. Rudnick, "Geometric Formulas for Dilution of Precision Calculations", *Navigation: Journal of The Institute of Navigation*, Vol. 37, No. 4, 1990, pp. 380-381.
- ¹¹G.A. Korn, T.M. Korn, *Mathematical Handbook for Scientists and Engineers*, 2nd ed., McGraw-Hill Book Company, 1968, p. 62.
- ¹²K. Rektorys (ed.), *Survey of Applicable Mathematics*, The M.I.T. Press, 1969, p. 238.
- ¹³G.A. Korn, T.M. Korn, *Mathematical Handbook for Scientists and Engineers*, 2nd ed., McGraw-Hill Book Company, 1968, p. 894.
- ¹⁴P.S. Noe, K.A. Myers, T.K. Wu, "A Navigation Algorithm for the Low-Cost Receiver", *Navigation: Journal of The Institute of Navigation*, Vol. 25, No. 2, 1978, pp. 258-264.
- ¹⁵P. Axelrad, J. Kelley, "Near Earth Orbit Determination and Rendezvous Navigation Using GPS", *Position Location and Navigation Symposium*, 1986, pp. 184-191.

- ¹⁶Jorge Galdos, Triveni N. Upadhyay, A. Wayne Deaton, James J. Lomas, "GPS Relative Navigation Filter for Automatic Rendezvous and Capture", *Proceedings of the National Technical Meeting of the Institute of Navigation*, 1993, pp. 83-94.
- ¹⁷M.S. Braasch, "A Signal Model for GPS", *Navigation: Journal of The Institute of Navigation*, Vol. 37, No. 4, 1990, pp. 363-377.
- ¹⁸M.S. Braasch, A. Fink, K. Duffus, "Improved Modeling of GPS Selective Availability", *Proceedings of the National Technical Meeting of the Institute of Navigation*, 1993, pp. 121-130.
- ¹⁹B. Hofmann-Wellenhof, H. Lichtenegger, J. Collins, *GPS: Theory and Practice*, 1st ed., Springer-Verlag, 1993.
- ²⁰A. Gelb (ed.), *Applied Optimal Estimation*, The M.I.T. Press, 1974.
- ²¹J. R. Wertz, W.J. Larson (eds.), *Space Mission Analysis and Design*, Kluwer Academic Publishers, 1991, p. 127.
- ²²A. Gelb (ed.), *Applied Optimal Estimation*, The M.I.T. Press, 1974.
- ²³Patrick Y.C. Hwang, "Kinematic GPS: Resolving Integer Ambiguities on the Fly", *Position Location and Navigation Symposium*, 1990.
- ²⁴Patrick Y.C. Hwang, "Kinematic GPS: Resolving Integer Ambiguities on the Fly", *Position Location and Navigation Symposium*, 1990, p. 580.
- ²⁵B.W. Remondi, "Performing Centimeter Level Surveys in Seconds with GPS Carrier Phase: Initial Results", *Navigation: Journal of the Institute of Navigation*, Vol. 32, No. 4, Winter 1985-86.
- ²⁶R. Grover Brown, Patrick Y.C. Hwang, "A Kalman Filter Approach to Precision GPS Geodesy", *Navigation: Journal of the Institute of Navigation*, Vol. 30, No. 4, 1983-84.
- ²⁷Patrick Y.C. Hwang, "Kinematic GPS: Resolving Integer Ambiguities on the Fly", *Position Location and Navigation Symposium*, 1990.
- ²⁴Patrick Y.C. Hwang, "Kinematic GPS: Resolving Integer Ambiguities on the Fly", *Position Location and Navigation Symposium*, 1990, pp. 583-584.
- ²⁹Alan S. Hope, "Ground Test of Satellite Attitude Determination Using GPS", *AAS/AIAA Spaceflight Mechanics Meeting*, Cocoa Beach, Florida, February 14-16, 1994.

- ³⁰R. Grover Brown, Patrick Y.C. Hwang, "A Kalman Filter Approach to Precision GPS Geodesy", *Navigation: Journal of the Institute of Navigation*, Vol. 30, No. 4, 1983-84.
- ³¹Patrick Y.C. Hwang, "Kinematic GPS: Resolving Integer Ambiguities on the Fly", *Position Location and Navigation Symposium*, 1990, p. 584.
- ³²E.G. Lightsey, C.E. Cohen, B.W. Parkinson, "Mitigating Multipath Error in GPS Based Attitude Determination", *AAS Guidance and Control Conference*, Keystone, Colorado, Feb. 1991.
- ³³E.G. Lightsey, C.E. Cohen, B.W. Parkinson, "Application of GPS Attitude Determination to Gravity Gradient Stabilized Spacecraft", *AIAA Guidance, Navigation, and Control Conference*, Monterey, CA, Aug. 1993, p. 821.
- ³⁴E.G. Lightsey, C.E. Cohen, B.W. Parkinson, "Application of GPS Attitude Determination to Gravity Gradient Stabilized Spacecraft", *AIAA Guidance, Navigation, and Control Conference*, Monterey, CA, Aug. 1993.
- ³⁵P.J. Melvin, A.S. Hope, "Satellite Attitude Determination with GPS", *AAS/AIAA Astrodynamics Specialist Conference*, Victoria, Canada, August 16-19, 1993.
- ³⁶E.G. Lightsey, C.E. Cohen, B.W. Parkinson, "Application of GPS Attitude Determination to Gravity Gradient Stabilized Spacecraft", *AIAA Guidance, Navigation, and Control Conference*, Monterey, CA, Aug. 1993.
- ³⁷P.J. Melvin, A.S. Hope, "Satellite Attitude Determination with GPS", *AAS/AIAA Astrodynamics Specialist Conference*, Victoria, Canada, August 16-19, 1993.
- ³⁸P.J. Melvin, A.S. Hope, "Satellite Attitude Determination with GPS", *AAS/AIAA Astrodynamics Specialist Conference*, Victoria, Canada, August 16-19, 1993, p. 13.
- ³⁹J. R. Wertz, W.J. Larson (eds.), *Space Mission Analysis and Design*, Kluwer Academic Publishers, 1991, pp. 303-329.
- ⁴⁰Marshall H. Kaplan, *Modern Spacecraft Dynamics and Control*, John Wiley & Sons, New York, 1976, pp. 199-204.
- ⁴¹E.G. Lightsey, C.E. Cohen, B.W. Parkinson, "Application of GPS Attitude Determination to Gravity Gradient Stabilized Spacecraft", *AIAA Guidance, Navigation, and Control Conference*, Monterey, CA, Aug. 1993.
- ⁴²G. Brondino, J. Legenne, "Hermes Guidance, Navigation, and Control System For Rendezvous Phases", Proc. First ESA Internat. Conf. on Spacecraft Guidance, Navigation, and Control Systems, Noordwijk, The Netherlands, June 1991.

REPORT DOCUMENTATION PAGE			Form Approved OMB No. 0704-0188	
Public reporting burden for this collection of information is estimated to average 1 hour per response, including the time for reviewing instructions, searching existing data sources, gathering and maintaining the data needed, and completing and reviewing the collection of information. Send comments regarding this burden estimate or any other aspect of this collection of information, including suggestions for reducing this burden, to Washington Headquarters Services, Directorate for Information Operations and Reports, 1215 Jefferson Davis Highway, Suite 1204, Arlington, VA 22202-4302, and to the Office of Management and Budget, Paperwork Reduction Project (0704-0188), Washington, DC 20503.				
1. AGENCY USE ONLY (Leave blank)	2. REPORT DATE July 1994	3. REPORT TYPE AND DATES COVERED Contractor Report		
4. TITLE AND SUBTITLE Evaluation of GPS Position and Attitude Determination for Automated Rendezvous and Docking Missions			5. FUNDING NUMBERS NCC1-104 WU 225-99-00-01	
6. AUTHOR(S) Marc D. DiPrinzio and Robert H. Tolson				
7. PERFORMING ORGANIZATION NAME(S) AND ADDRESS(ES) The George Washington University Joint Institute for Advancement of Flight Sciences NASA Langley Research Center Hampton, VA 23681-0001			8. PERFORMING ORGANIZATION REPORT NUMBER	
9. SPONSORING/MONITORING AGENCY NAME(S) AND ADDRESS(ES) National Aeronautics and Space Administration Langley Research Center Hampton, VA 23681-0001			10. SPONSORING/MONITORING AGENCY REPORT NUMBER NASA CR-4614	
11. SUPPLEMENTARY NOTES The information presented in this report was offered as a thesis by the first author in partial fulfillment of the requirements for the Degree of Master of Science, The George Washington University, June 1994. Langley Technical Monitor: Stephen J. Katzberg				
12a. DISTRIBUTION/AVAILABILITY STATEMENT Unclassified - Unlimited Subject Category 18			12b. DISTRIBUTION CODE	
13. ABSTRACT (Maximum 200 words) The use of the Global Positioning System for position and attitude determination is evaluated for an automated rendezvous and docking mission. The typical mission scenario involves the chaser docking with the target for resupply or repair purposes, and is divided into three sections. During the homing phase, the chaser utilizes Coarse Acquisition pseudorange data to approach the target; guidance laws for this stage are investigated. In the second phase, differential carrier phase positioning is utilized. The chaser must maintain a quasi-constant distance from the target, in order to resolve the initial integer ambiguities. Once the ambiguities are determined, the terminal phase is entered, and the rendezvous is completed with continuous carrier phase tracking. Attitude knowledge is maintained in all phases through the use of the carrier phase observable. A Kalman filter is utilized to estimate all states from the noisy measurement data. The effects of Selective Availability and cycle slips are also investigated.				
14. SUBJECT TERMS Global Positioning System; Rendezvous simulation; Kalman filter; Carrier phase			15. NUMBER OF PAGES 85	
			16. PRICE CODE A05	
17. SECURITY CLASSIFICATION OF REPORT Unclassified	18. SECURITY CLASSIFICATION OF THIS PAGE Unclassified	19. SECURITY CLASSIFICATION OF ABSTRACT Unclassified	20. LIMITATION OF ABSTRACT	